IJMMM International Journal of Minerals, Metallurgy and Materials 矿物冶金与材料学报（英文版）

Research progress of CO_2 capture and mineralization based on natural minerals

Chenguang Qian, Chunquan Li, Peng Huang, Jialin Liang, Xin Zhang, Jifa Wang, Jianbing Wang, and Zhiming Sun

Cite this article as:
Chenguang Qian, Chunquan Li, Peng Huang, Jialin Liang, Xin Zhang, Jifa Wang, Jianbing Wang, and Zhiming Sun, Research progress of CO_2 capture and mineralization based on natural minerals, *Int. J. Miner. Metall. Mater.*, 31(2024), No. 6, pp. 1208-1227. https://doi.org/10.1007/s12613-023-2785-4

View the article online at SpringerLink or IJMMM Webpage.

Articles you may be interested in

Meng-jun Hu, Ming-zhu Yin, Li-wen Hu, Peng-jie Liu, Shuo Wang, and Jian-bang Ge, High-value utilization of CO_2 to synthesize sulfur-doped carbon nanofibers with excellent capacitive performance, *Int. J. Miner. Metall. Mater.*, 27(2020), No. 12, pp. 1666-1677. https://doi.org/10.1007/s12613-020-2120-2

Hui-xin Li, Da-peng Li, Lei Zhang, Ya-wen Wang, Xiu-yun Wang, and Min-xu Lu, Passivity breakdown of 13Cr stainless steel under high chloride and CO_2 environment, *Int. J. Miner. Metall. Mater.*, 26(2019), No. 3, pp. 329-336. https://doi.org/10.1007/s12613-019-1741-9

Jin-yang Zhu, Li-ning Xu, Min-xu Lu, and Wei Chang, Cathodic reaction mechanisms in CO_2 corrosion of low-Cr steels, *Int. J. Miner. Metall. Mater.*, 26(2019), No. 11, pp. 1405-1414. https://doi.org/10.1007/s12613-019-1861-2

Zhi-yu Chang, Ping Wang, Jian-liang Zhang, Ke-xin Jiao, Yue-qiang Zhang, and Zheng-jian Liu, Effect of CO_2 and H_2O on gasification dissolution and deep reaction of coke, *Int. J. Miner. Metall. Mater.*, 25(2018), No. 12, pp. 1402-1411. https://doi.org/10.1007/s12613-018-1694-4

Min-min Sun, Jian-liang Zhang, Ke-jiang Li, Ke Guo, Zi-ming Wang, and Chun-he Jiang, Gasification kinetics of bulk coke in the $CO_2/CO/H_2/H_2O/N_2$ system simulating the atmosphere in the industrial blast furnace, *Int. J. Miner. Metall. Mater.*, 26(2019), No. 10, pp. 1247-1257. https://doi.org/10.1007/s12613-019-1846-1

Hui-bin Wu, Tao Wu, Gang Niu, Tao Li, Rui-yan Sun, and Yang Gu, Effect of the frequency of high-angle grain boundaries on the corrosion performance of 5wt%Cr steel in a CO_2 aqueous environment, *Int. J. Miner. Metall. Mater.*, 25(2018), No. 3, pp. 315-324. https://doi.org/10.1007/s12613-018-1575-x

IJMMM WeChat

QQ author group

INTERNATIONAL JOURNAL OF
Minerals, Metallurgy and Materials

Volume 31, Number 6, June 2024
Page 1208

Invited Review https://doi.org/10.1007/s12613-023-2785-4

Research progress of CO_2 capture and mineralization based on natural minerals

Chenguang Qian[1)], *Chunquan Li*[1)], *Peng Huang*[2)], *Jialin Liang*[1)], *Xin Zhang*[1)], *Jifa Wang*[1)], *Jianbing Wang*[1),✉], *and Zhiming Sun*[1),✉]

1) School of Chemical and Environmental Engineering, China University of Mining and Technology (Beijing), Beijing 100083, China
2) Shanghai Construction Building Material Technology Group, Shanghai 200080, China

(Received: 10 May 2023; revised: 8 November 2023; accepted: 17 November 2023)

Abstract: Natural minerals, such as kaolinite, halloysite, montmorillonite, attapulgite, bentonite, sepiolite, forsterite, and wollastonite, have considerable potential for use in CO_2 capture and mineralization due to their abundant reserves, low cost, excellent mechanical properties, and chemical stability. Over the past decades, various methods, such as those involving heat, acid, alkali, organic amine, amino silane, and ionic liquid, have been employed to enhance the CO_2 capture performance of natural minerals to attain high specific surface area, a large number of pore structures, and rich active sites. Future research on CO_2 capture by natural minerals will focus on the full utilization of the properties of natural minerals, adoption of suitable modification methods, and preparation of composite materials with high specific surface area and rich active sites. In addition, we provide a summary of the principle and technical route of direct and indirect mineralization of CO_2 by natural minerals. This process uses minerals with high calcium and magnesium contents, such as forsterite (Mg_2SiO_4), serpentine [$Mg_3Si_2O(OH)_4$], and wollastonite ($CaSiO_3$). The research status of indirect mineralization of CO_2 using hydrochloric acid, acetic acid, molten salt, and ammonium salt as media is also introduced in detail. The recovery of additives and high-value-added products during the mineralization process to increase economic benefits is another focus of future research on CO_2 mineralization by natural minerals.

Keywords: natural mineral; carbon dioxide capture; modification; composite material; carbon dioxide mineralization

1. Introduction

Over the centuries, human actions have resulted in a continual increase in the average atmospheric concentration of CO_2, which rose from less than 280 ppm before the Industrial Revolution to 418 ppm in 2022 (Fig. 1(a)) [1–2]. In general, CO_2 emissions are caused by the burning of fossil fuels, such as coal, oil, and natural gas (Fig. 1(b)) [2]. CO_2 concentration has consistently increased by approximately 2.3 ppm/year in the previous decade. If CO_2 emissions remain unregulated, the concentration of CO_2 in the atmosphere will exceed 500 ppm by 2050 [3]. Considerable CO_2 emissions result in global warming, which in turn triggers a host of issues, including the melting of glaciers, acidification of oceans, rise in sea levels, extinction of various animal and plant species, frequent extreme weather, and rampant disease [4–7]. Global warming has a notable influence on social, economic, and human survival and development [8].

Many countries are committed to the development of hydropower, nuclear power, wind power, hydrogen, and other clean energy. The energy structure dominated by fossil fuels, such as coal, oil, and natural gas, will remain unchanged for a long time in the future, and the avoidance of considerable amounts of CO_2 emissions will be difficult [9–10]. In this context, carbon capture utilization and storage (CCUS/CCS) technologies have been proposed and used to mitigate CO_2 emissions [11–18]. CCUS/CCS technology involves the separation of CO_2 emissions from the industry and related energy industries through carbon capture technology. The captured CO_2 is then either stored or utilized to reduce CO_2 emission (Fig. 2) [19]. CCUS/CCS technology can achieve widespread low-carbon utilization of fossil energy, and it has attracted great attention from the international community. In addition, CCUS/CCS technology is the most direct and effective measure for the control of CO_2 emissions in the world and will be widely used in power generation and other industries in the future [20–22]. By 2050, 7 billion tons of CO_2 is expected to be sequestered annually [23].

Carbon capture technology separates CO_2 from industrial waste gas to obtain high-purity CO_2. Based on the different coupling positions in the combustion process, capture methods are divided into three categories: pre-combustion capture, post-combustion capture, and oxygen-enriched combustion (Fig. 3) [12,23–24]. Pre-combustion and oxyfuel combustion

---

✉ Corresponding authors: Jianbing Wang E-mail: wangjb@cumtb.edu.cn; Zhiming Sun E-mail: zhimingsun@cumtb.edu.cn

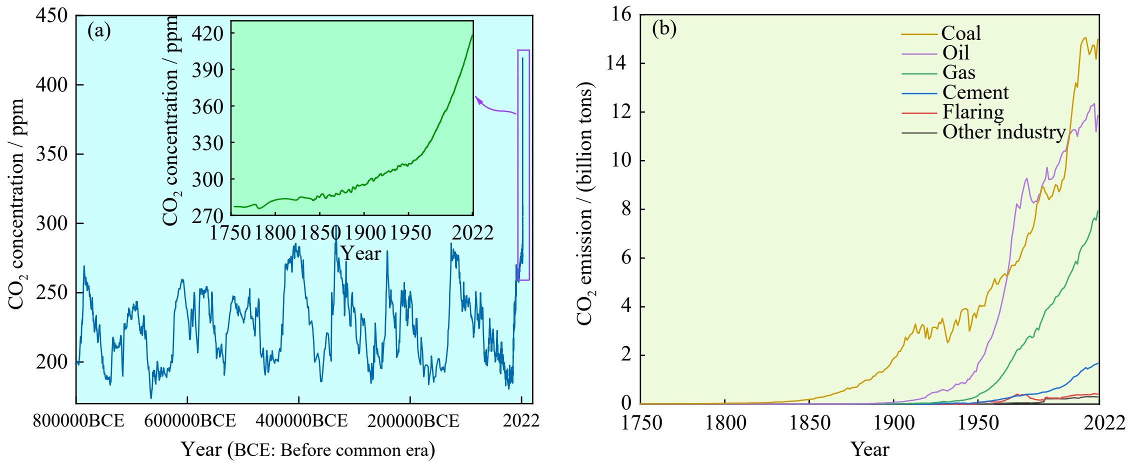

Fig. 1. (a) Global atmospheric CO_2 concentrations over 800000 years; (b) changes in global CO_2 emissions from 1750 to 2022 depending on the fuel type [2].

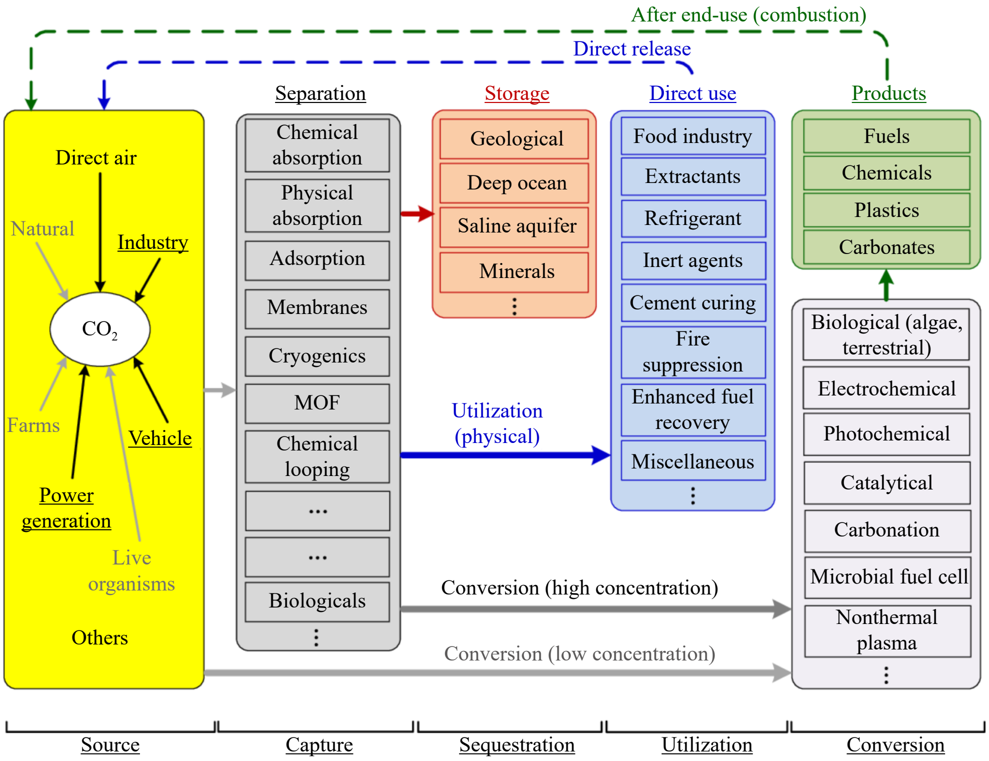

Fig. 2. Carbon capture, storage, utilization, and conversion [19].

contains high concentrations of CO_2, which can be directly used or stored. The flue gas obtained after combustion has the characteristics of low pressure, low CO_2 concentration, and high N_2 content. Thus, high-concentration CO_2 can be obtained by carbon capture technology [25].

Flue gas after combustion can be captured using methods such as absorption, solid adsorption, membrane separation, cryogenic separation, and hypergravity. Absorption occurs as physical and chemical absorption [26–27]. Physical absorption is dependent on water, methanol, propylene carbonate, and other solutions as absorbents. According to Henry’s law, the solubility of CO_2 in solution changes with the pressure to absorb or desorb [28]. Chemical absorption refers to the absorption of CO_2 through acid–base reaction [14]. Membrane separation separates specific gases from mixed ones by utilizing the pressure difference on both sides of a membrane as the separation power or permeability difference of certain polymer membranes to distinguish gases [29]. Solid adsorption utilizes the van der Waals force between CO_2 molecules and adsorbents to adsorb and desorb CO_2 under various temperatures and pressure conditions. This method has the advantages of low energy consumption and corrosion, simple process, high stability, and environmental protection [30–31]. Given the adsorption–desorption temperature of solid materials, solid adsorbents can be divided into low, medium, and high-temperature capture materials [2]. The capture materials in the low-temperature region (<473 K) mainly include metal–organic frameworks (MOFs), zeolites, porous carbon

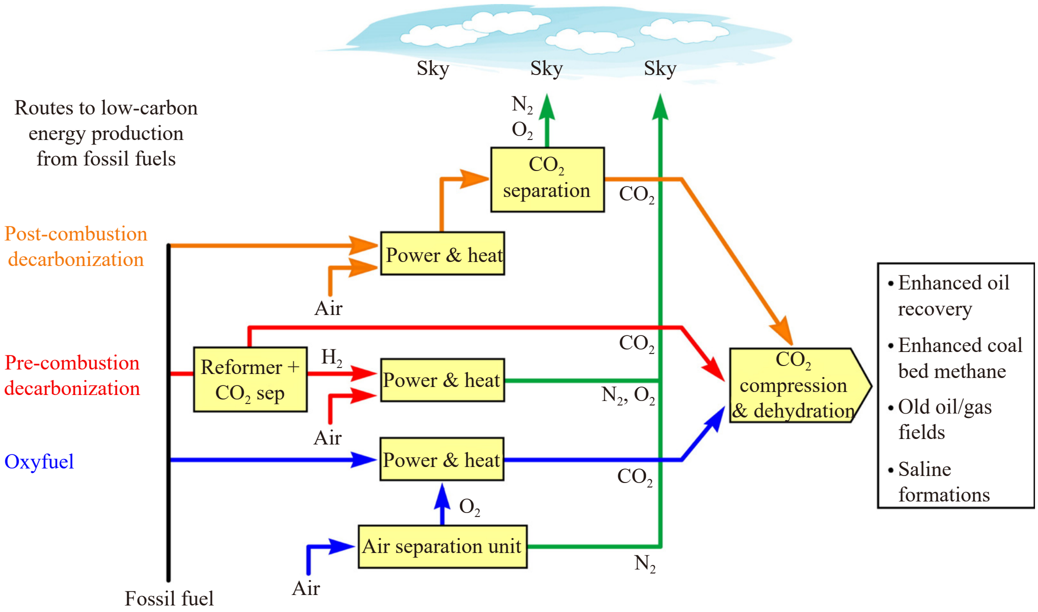

Fig. 3. CO_2 capture methods [23]. Reprinted from *J. Membr. Sci.*, Vol. 359, T.C. Merkel, H.Q. Lin, X.T. Wei, and R. Baker, Power plant post-combustion carbon dioxide capture: An opportunity for membranes, 126-139, Copyright 2010, with permission from Elsevier.

materials, mesoporous silica, porous organic polymers, and natural minerals [25,32–35]. The middle-temperature region (473–673 K) mainly contains capture materials, including metal oxides and hydrotalcite-like compounds [36]. The high-temperature region (>673 K) mainly comprises capture materials including lithium zirconate, natural minerals with high calcium and magnesium content, and industrial solid waste (Fig. 4) [2,37–39]. These solid adsorbents can be utilized in CO_2 capture at different temperatures. Natural minerals are exceptional solid adsorption matrix materials due to their plentiful reserves, low cost, high specific surface area, rich pore structure, excellent mechanical properties, and chemical stability [40].

Rather than releasing it into the atmosphere, carbon sequestration technology captures, compresses, and transports the CO_2 generated by large emission sources to select sites for long-term storage. CO_2 storage methods mainly consist of geological storage, marine storage, mineral storage (also known as mineralization), etc. [41]. Geological and marine storage are effective methods for CO_2 storage; however, these come with risks of carbon dioxide leakage, groundwater pollution, geological disaster, seawater acidification, ecological imbalance, and other risks in the storage process [42–43]; notably, mineralization overcomes these shortcomings [20]. CO_2 mineralization refers to the simulation and acceleration of the weathering process of rocks in nature, with

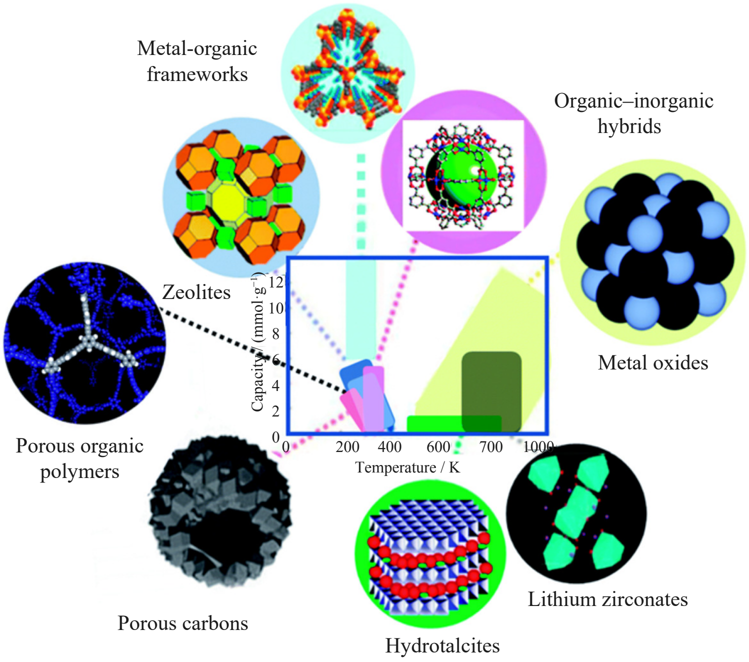

Fig. 4. Solid adsorbents and relevant relationships between capacity and temperature [2].

CO_2 used to react with natural minerals containing calcium and magnesium and form stable carbonates ($CaCO_3$/$MgCO_3$) (Fig. 5) [42,44]. The formation of stable carbonates through CO_2 mineralization prevents the harm caused by CO_2 leakage in the later stage. Mineralization shows better stability than other storage methods, and the mineralized products have a certain recycling value [45]. In addition, natural minerals, which have gradually become the focus of current research, play a crucial role in CO_2 capture and mineralization [46]. This paper reviews the research on CO_2 capture and mineralization by natural minerals. Various methods for enhancing the CO_2 capture and mineralization performance of natural minerals are also introduced.

2. CO_2 capture by natural minerals

Natural minerals play an important role in CO_2 capture, utilization, and mineralization due to their plentiful reserves, low cost, excellent mechanical properties, and chemical stability. CO_2 capture frequently involves the use of minerals, such as kaolinite, halloysite, montmorillonite, bentonite, attapulgite, sepiolite, etc. The capture of CO_2 by these minerals primarily occurs through physical adsorption; however, their adsorption capacity is relatively limited [47]. Therefore, the CO_2 capture capability of natural minerals must be improved via different modification strategies [25].

2.1. CO_2 capture by unmodified natural minerals

In general, CO_2 adsorption onto the surface and interior of natural minerals occurs via physical adsorption or chemical reactions. The adsorption capacity of CO_2 is influenced by crystal structure, specific surface area, pore structure, ion exchange, and other properties of minerals. Table 1 shows the CO_2 adsorption capacity of natural minerals.

The mineral known as kaolinite ($Al_4[Si_4O_{10}](OH)_8$) is a typical 1:1 octahedral layered clay mineral consisting of a SiO_4 tetrahedron layer and an $AlO_2(OH)_4$ layer [49]. Strong hydrogen bonds tightly connect the interlayer, resulting in low CO_2 adsorption capacity due to the dominant physical adsorption [59]. Meanwhile, halloysite ($Al_2Si_2O_5(OH)_4 \cdot nH_2O$) is a polytype of kaolinite with a multiwalled nanotubular structure. The outer surface comprises tetrahedral groups containing silicon–oxygen groups (Si–O–Si), and the inner wall consists of octahedral aluminum hydroxyl groups (Al–OH) [60–61]. This mineral has high specific surface area, developed pore structure, and rich active groups, which

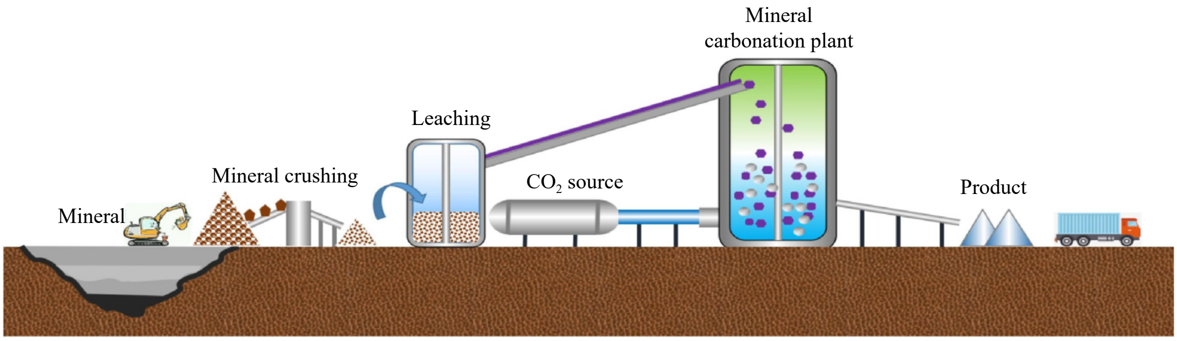

Fig. 5. Schematic of CO_2 mineral storage [42]. Reprinted from *Chem. Eng. J.*, Vol. 416, W.Z. Liu, L.M. Teng, S. Rohani, *et al.*, CO_2 mineral carbonation using industrial solid wastes: A review of recent developments, 129093, Copyright 2021, with permission from Elsevier.

Table 1. CO_2 adsorption capacity of natural minerals

Support	Adsorption conditions			CO_2 uptake / ($mmol \cdot g^{-1}$)	Ref.
	Temperature / °C	Gas atmosphere	Pressure / MPa		
Kaolinite	0	CO_2	3	0.29	[48]
	25		3	0.14	[48]
	25		0.1	0.06	[49]
	15		1.7	0.14	[50]
Halloysite	0	CO_2	3	6.17	[51]
	75		0.1	0.08	[52]
Bentonite	25	CO_2	0.1	0.13	[53]
	30			0.14	[54]
Montmorillonite	25	CO_2	0.1	0.16	[55]
	45			0.22	[56]
Palygorskite	45	CO_2	0.1	0.27	[56]
	25			0.40	[57]
Sepiolite	45	CO_2	0.1	0.93	[56]
	50			0.41	[58]

are conducive to CO_2 adsorption. Montmorillonite ($(Na,Ca)_{0.33}(Al,Mg)_2[Si_4O_{10}](OH)_2\cdot nH_2O$) is a layered aluminosilicate with a 2:1 structure, and it consists of two silicon–oxygen tetrahedron layers and one aluminum–oxygen octahedron layer. Compared with that of kaolinite, the interlayer of montmorillonite is more prone to relative sliding. Montmorillonite exhibits a natural nanosheet morphology, high porosity, and good cation exchange, and it has a slightly higher CO_2 adsorption capability than kaolinite [62]. Attapulgite ($Mg_5Si_8O_{20}(OH)_2(OH_2)_4\cdot 4H_2O$) or palygorskite recognized through its 2:1 layered chain structure composed of a silicon–oxygen tetrahedral layer and a discontinuously arranged octahedral layer. This natural magnesium–aluminum-rich clay mineral is known for its rich pores, large specific surface area, and high porosity, which can be attributed to its unique fibrous, chain, rod-like microstructure, and nanoproperties. Moreover, attapulgite contains numerous oxygen-containing functional groups, which are evenly distributed on its surface and enhance the interaction between adsorbents and CO_2 [63]. Sepiolite ($Si_{12}Mg_8O_{30}(OH)_4(OH_2)_4\cdot 8H_2O$) is a lightweight hydrated magnesium silicate clay mineral. This mineral possesses a nanofiber structure and a high number of silane alcohol groups, uniform pore size, high porosity, and large specific surface area, which can enhance CO_2 adsorption [64].

2.2. CO_2 capture by modified natural minerals

To enhance the adsorption capability of natural minerals to CO_2, scientists treat them by using common treatment methods, including pretreatment (heat, acid, alkali, etc.), organic amine, ionic liquid (IL), pillared or metal-doped modification, etc.

2.2.1. Pretreatment

In the production of solid CO_2 adsorbents, natural minerals must first be treated with heat, acids, and alkali, to further improve their purity, increase their specific surface area, and enhance their pore structure to increase the number of CO_2 adsorption sites and reaction cavities. Table 2 reveals the changes in structural and adsorption properties of materials after the treatment of natural minerals by heat, acids, and alkali.

Heat treatment increases a material's specific surface area and pore structure [68]. Its treatment effect mainly depends on the temperature and adsorbate properties. This process can be used as a pretreatment step in combination with acid or alkali treatment. Niu *et al.* [66] first calcined halloysite in air at 850°C for 4 h and added the calcined halloysite with 6 mol/L hydrochloric acid; the specific surface area of the treated halloysite increased from 63.4 to 366.4 m^2/g, which can provide more organic amine loading sites. Acid treatment (e.g., HCl, H_2SO_4, and HNO_3) can be used to leach metal cations (such as Al^{3+}, Mg^{2+}, Fe^{3+}, Na^+, etc.) and impurities in natural minerals, considerably increase the specific surface area and pore volume, and improve structural properties, thereby increasing the adsorption performance of CO_2 [47]. Zhu *et al.* [58] applied hydrochloric acid treatment of sepiolite; as a result, hydrogen ions replaced magnesium ions, and a large amount of Si–OH was produced on the pore wall of the mineral. An increase in the specific surface area was observed from 79 m^2/g before acid treatment to 182 m^2/g afterward. The adsorption capacity of CO_2, mainly physical adsorption, increased from 0.41 to 0.65 mmol/g. Ouyang *et al.* [67] conducted the pretreatment of sepiolite using 4 mol/L hydrochloric acid; they observed that the specific surface area of the treated sepiolite reached up to 320 m^2/g, which was eight times higher than that of pristine sepiolite; moreover, the adsorption of CO_2 was enhanced from 0.30 to 0.50 mmol/g at 70°C. Compared with acid treatment, metal cations may be

Table 2. Structural and adsorption properties of natural mineral-pretreated materials

Supports	Pretreatment	Structure property		Adsorption conditions			CO_2 uptake / $(mmol\cdot g^{-1})$	Ref.
		Specific surface area / $(m^2\cdot g^{-1})$	Pore volume / $(cm^3\cdot g^{-1})$	Temperature / °C	Gas atmosphere	Pressure / MPa		
Kaolinite	Without pretreatment	8	0.01	—	—	—	—	[65]
	6 M HCl, 4 h	38	0.07					
	5 M NaOH, 4 h	16	0.03					
Halloysite	Without pretreatment	63.4	0.24	—	—	—	—	[66]
	850°C, 4 h + 6 M HCl, 6 h	366.4	0.55					
Bentonite	Without pretreatment	81	0.10	30	CO_2	0.1	0.14	[54]
	3 M HCl, 3 h	227	0.31				0.34	
Montmorillonite	Without pretreatment	72	0.16	—	—	—	—	[65]
	6 M HCl, 4 h	253	0.71					
	5 M NaOH, 4 h	183	0.56					
Sepiolite	Without pretreatment	79	0.01	50	CO_2	0.1	0.41	[58]
	2 M HCl, 24 h	182	0.21				0.65	
	Without pretreatment	42.74	0.08	75	CO_2	0.1	0.27	[64]
	2 M HCl, 6 h	168.96	0.14				0.41	
	Without pretreatment	42.74	—	70	CO_2	0.1	0.30	[67]
	4 M HCl, 6 h	320.31					0.50	

inert in alkali treatment (such as NaOH), which results in the poor modification effect of natural minerals [65]. In addition, appropriate heat treatment temperature and acid/alkali concentration are required in the pretreatment of natural minerals using heat, acid, alkali, and other methods. Excessive acid and alkali concentrations and high heat treatment temperatures may damage the structure of natural minerals, thus affecting CO_2 adsorption properties.

2.2.2. Organic amine impregnation modification

Organic amine absorbents enable the chemical interaction between amine groups in molecules and CO_2. Therefore, the application of these absorbents in CO_2 capture is one of the most effective methods for enhancing CO_2 capture in the industry [69–70]. The commonly used organic amine absorbents include amine alcohols (monoethanolamine (MEA), diethanolamine (DEA), and methyl diethanolamine (MDEA), aliphatic amines (ethylenediamine (EDA), tetraethylenepentamine (TEPA), hexylamine (HXA), dodecylamine (DDA), and octadecyl amine (ODA)), amides (pentavinylacetamide (PEHA) and formamides), and other amines (polyethyleneimine (PEI)). However, as a result of equipment corrosion, solvent degradation, and high energy-intensive regeneration during the use of organic amine absorbents, their application in the industry faces enormous challenges [71–73]. Researchers have proposed the inclusion of amine-based absorbents with an affinity for CO_2 into the structures of natural minerals through the physical leaching method to increase the mass transfer and rapid adsorption of CO_2 [48,64,66,74–75] (Fig. 6); this method improves the CO_2 capture capacity of amine-based composite solid adsorbents and reduces energy consumption during the adsorbent regeneration process [76]. The CO_2 adsorption capacity of organic amine-functionalized natural minerals can be found in Table 3.

For the enhanced adsorption capacity of aminated mineral-based solid adsorbents, the effective adsorption area of minerals and the active sites per unit area must be increased, and appropriate adsorption conditions must be selected [25]. The specific surface area and porosity of solid adsorbents depend on the type and pretreatment method of natural minerals, thus affecting the adsorption area. To a certain extent, the number of active sites of adsorbents depends on the type of organic amine, length of alkyl amine molecular chain, and loading amount. The sufficient contact and reaction between CO_2 and aminated solid adsorbents can be guaranteed by appropriate adsorption conditions (such as CO_2 flow rate, adsorption temperature, pressure, and water content).

The type of organic amine greatly influences the CO_2 adsorption performance. Chen and Lu [49] explored the effect of different amine-modified kaolinite on the adsorption performance of CO_2. MEA, EDA, and 4MEA + 1EDA were loaded on kaolinite via immersion method, and adsorption was carried out at the adsorption temperature of 25°C and CO_2 flow rate of 30 mL/min. The results show that the CO_2

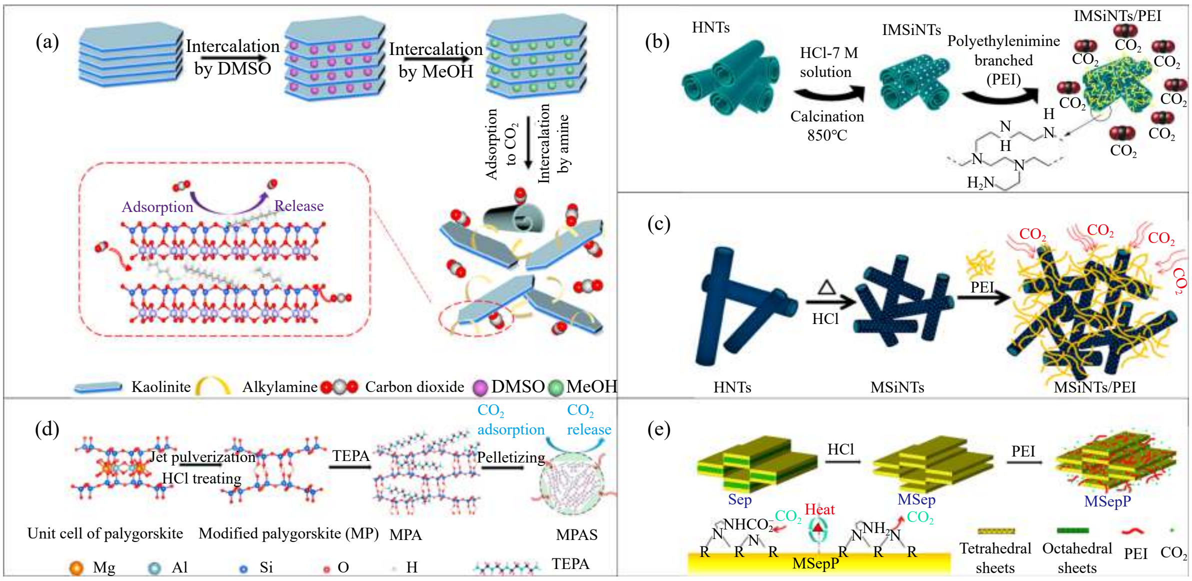

Fig. 6. **(a) Amine-modified kaolinite after intercalation [48]; (b) modification of acid and calcined halloysite with PEI (IMSiNTs: improved mesoporous silica nanotubes) [74]; (c) modified acid-treated halloysite with PEI [66]; (d) modified acid-treated palygorskite (MPA) with TEPA (MPAS: MPA spheres) [75]; (e) modified acid-treated sepiolite (Sep) with PEI (MSepP: Sep/PEI) [64]. (a) Reprinted from *Appl. Clay Sci.*, Vol. 228, Q.H. Liu, J.L. Jiang, F. Zhang, *et al.*, CO_2 fixation mechanism of kaolin treated with organic amines at varied temperatures and pressure, 106638, Copyright 2022, with permission from Elsevier. (b) Reprinted with permission from F.S. Taheri, A. Ghaemi, A. Maleki, and S. Shahhosseini, *Energy Fuels*, vol. 33, 5384-5397 (2019) [74]. Copyright 2019 American Chemical Society. (c) Reprinted with permission from M.Y. Niu, H.M. Yang, X.C. Zhang, Y.T. Wang, and A.D. Tang, *ACS Appl. Mater. Interfaces*, vol. 8, 17312-17320 (2016) [66]. Copyright 2016 American Chemical Society. (d) Reprinted from *Chem. Eng. J.*, Vol. 341, J. Ouyang, W. Gu, Y. Zhang, *et al.*, CO_2 capturing performances of millimeter scale beads made by tetraethylenepentamine loaded ultra-fine palygorskite powders from jet pulverization, 432-440, Copyright 2018, with permission from Elsevier. (e) Reprinted from *Appl. Clay Sci.*, Vol. 152, J. Ouyang, W. Gu, C.H. Zheng, *et al.*, Polyethyleneimine (PEI) loaded MgO–SiO$_2$ nanofibers from sepiolite minerals for reusable CO_2 capture/release applications, 267-275, Copyright 2018, with permission from Elsevier.**

Table 3. CO_2 adsorption capacity of natural minerals functionalized by organic amines

Support	Pretreatment	Amine loading / wt%	Adsorption conditions			Regeneration conditions		Cycle number	CO_2 uptake / ($mmol \cdot g^{-1}$)		Loss / %	Ref.
			Temperature / °C	Atmosphere	Pressure / MPa	Temperature / °C	Atmosphere		X	$X_{residue}$		
Kaolinite	Intercalation	6.35 (HXA) 12.6 (DDA) 41.7 (ODA)	0	CO_2	3	105	N_2	—	0.75 0.50 0.28	—	—	[48]
	Without pretreatment	20 (MEA) 33.3 (EDA) 50 (4MEA–1EDA)	25	CO_2	0.1	100	N_2	—	2.94 1.35 3.38	—	—	[49]
Halloysite	Without pretreatment	44.4 (Formamide)	0 25	CO_2	3	250	—	—	6.1 3.4	—	—	[51]
	Without pretreatment	30 (PEI)	75	CO_2	0.1	75	N_2	10	1.5	1.4	6.6	[52]
	Hydrochloric acid treatment	50 (PEI)	85	40vol%N_2 + 60vol%CO_2	0.1	110	N_2	10	2.75	2.66	3.2	[66]
	Hydrochloric acid treatment	30 (PEI)	25	Dry air	0.1	80	—	50	1.24	1.20	—	[77]
Palygorskite	Hydration treatment	37 (PEI)	45	CO_2	0.1	110	Ar	—	1.52	—	—	[56]
Sepiolite	Hydrochloric acid treatment	47 (PEHA)	50	CO_2 15vol%CO_2 + 85vol%N_2 (water content 5vol%)	0.1	105	N_2	10 —	2.47 2.94	2.23 —	9.8 —	[58]
	Hydrochloric acid treatment	50 (PEI)	75	40vol%N_2 + 60vol%CO_2	0.1	110	N_2	10	2.48	2.31	6.8	[64]
	Hydrochloric acid treatment	60 (TEPA)	60	1vol%CO_2 + 99vol%N_2 (water content 1vol%)	0.1	90	N_2	10	3.8	3.5	7.9	[78]
Bentonite	Without pretreatment	30 (PEI)	75	CO_2	0.1	75	He	5	1.06	1.02	3.7	[53]
	Sulfuric acid treatment	50 (TEPA)	75	CO_2 15vol%CO_2 + 4.5vol%O_2 + 80.5vol%N_2 (water content 18vol%)	0.1	100	N_2	10 —	2.54 4.31	2.43 —	4.3 —	[79]
Montmorillonite	Hydration treatment	37 (PEI)	45	CO_2	0.1	110	Ar	—	1.03	—	—	[56]
	Pillaring and calcination	60 (TEPA) 60 (PEI)	25	CO_2	0.1	—	—	—	1.64 1.45	—	—	[80]
	Hydrochloric acid treatment	50 (PEI)	75	CO_2 15vol%CO_2 + 4.5vol%O_2 + 80.5vol%N_2 (water content 3vol%)	0.1	100	N_2	10 —	2.54 3.23	2.43 —	4.4 —	[65]
	Without pretreatment	20–30 (ODA)	25	CO_2	5	—	—	—	7.16	—	—	[81]

Note: X—CO_2 uptake for fresh sample; $X_{residue}$—CO_2 uptake for cycle sample.

adsorption capacities of MEA, EDA, and 4MEA + 1EDA-modified kaolinite samples reached 2.94, 1.35, and 3.38 mmol/g, respectively. The chain length of alkylamine molecules also plays an important role in CO_2 adsorption. A small proportion of amine groups reacts with CO_2 in long-chain alkylamine molecules, whereas long-chain alkyl molecules may block the pores of adsorbents, which is not conducive to CO_2 diffusion. Liu *et al.* [48] explored the effect of molecular chain length on the CO_2 adsorption performance of intercalated kaolinite. First, kaolinite was intercalated with dimethyl sulfoxide (DMSO) to prepare K/DMSO, which was then dispersed in an HNO_3/methanol (MeOH) solution. After heating and washing, K/MeOH was prepared. Finally, HXA, DDA, and ODA were inserted into the modified kaolinite to improve the utilization rate of organic amines, and K/HXA, K/DDA, and K/ODA were prepared as adsorption materials (Fig. 6(a)). The results show the negative correlation of the adsorption capacity of the prepared adsorbent for pure CO_2 with the length of the alkylamine molecular chain (K/HXA > K/DDA > K/ODA); this finding indicates that the adsorption of kaolinite alkylamine on CO_2 was not simple physical adsorption, and NH_2 in the alkylamine molecule played a decisive role in the adsorption process. Nevertheless, excessive amine loading leads to mineral pore blockage and hinders CO_2 adsorption. Niu *et al.* [66] prepared a novel mesoporous silica nanotubes (MSiNTs)/PEI nanocomposite for CO_2 capture by impregnating acid-treated halloysite nanotubes (HNTs) with PEI (Fig. 6(c)). A thermogravimetric analyzer was used to analyze the effect of PEI loading on the adsorption capacity of the composite. The results showed that when the adsorption temperature was 50°C, the PEI loading was in the range of 30wt%–50wt%, and the adsorption capacity increased between 1.29–1.83 mmol/g. However, the CO_2 adsorption capacity decreased when the PEI loading reached 60wt%. Adsorption temperature and CO_2 pressure are also key factors affecting the adsorption capacity of materials. The adsorption temperature is determined based on the state of CO_2 to be adsorbed. Given the exothermic nature of the CO_2 adsorption process, the amount of CO_2 adsorbed at high temperatures is reduced [82]. Ramadass *et al.* [51] explored the effect of formamide-intercalated halloysite on the adsorption capacity for pure CO_2 at 0, 10, and 25°C, and a pressure of 3 MPa. The results indicate that the adsorption capacity of the intercalated halloysite adsorbent was 3.4 mmol/g at 25°C, and it increased to 6.1 mmol/g at 0°C. During CO_2 adsorption under normal pressure, an appropriate adsorption temperature benefits the improvement of amine activity and causes the appearance of amine active sites, which can also increase the diffusion of CO_2 in the pores, thereby improving the adsorption performance of the material. However, at extremely high adsorption temperatures, thermodynamics becomes dominant, and the equilibrium shifts to the desorption direction of CO_2, resulting in a decreased adsorption capacity of CO_2. Wang *et al.* [65] investigated the effect of PEI-impregnated montmorillonite on the adsorption performance of pure CO_2 at different adsorption temperatures of 30, 45, 60, 70, 80, and 85°C. The results show that the adsorption capacity of the material to CO_2 increased with the increase in adsorption temperature. The sample had a maximum adsorption capacity of 2.54 mmol/g at 75°C, but its adsorption capacity decreased when the adsorption temperature was continuously increased from 75 to 85°C. To simulate the performance of adsorbents in CO_2 capture in the actual industry, Zhu *et al.* [58] designed a fixed-bed reaction system (Fig. 7(a)) and used PEHA-impregnated acid-modified sepiolite as an adsorption material. Different CO_2 flow rates affect the CO_2 adsorption performance (Fig. 7(b)). An extremely low flow rate is not conducive to CO_2 diffusion in adsorbent materials, and an extremely high flow rate leads to transfer resistance between CO_2 molecules and active sites, which is not advantageous to the retention of CO_2 molecules in adsorbent materials. At a flow rate of 30 mL/min and an adsorption temperature of 50°C, experiments were conducted to determine the effect of water content on the adsorption performance of CO_2 for 15vol% CO_2 and 85vol% N_2 mixed gas. Studies have shown that an appropriate amount of water benefits the adsorption of CO_2, but when the water content exceeds 5vol%, the CO_2 adsorption reaction is inhibited (Fig. 7(c)). This phenomenon can be attributed to the excessive water molecules covering the pores and active sites of amines, and as a result, CO_2 molecules cannot bind to some amine sites, resulting in a decreased adsorption performance of the material.

Irani *et al.* [78] explored the effect of TEPA-modified sepiolite on CO_2 adsorption capacity under water-containing conditions. Studies have shown that the addition of 1vol% water benefits CO_2 adsorption, and the reaction mechanism of CO_2 under dry and wet conditions varies (Fig. 8). Under wet conditions, two bicarbonates can form between one CO_2 molecule and one amino group, and carbamate can form between two amino groups and one CO_2. However, only carbamate has been formed under dry CO_2 conditions [65,83].

2.2.3. Aminosilane grafting modification

Aminosilane grafting, which is more stable than organic amine leaching, is carried out using a chemical reaction between a silanol group on the mineral surface and an amine–alkoxysilane compound [54,84–85] (Fig. 9)). Stevens *et al.* [86] prepared diamine-modified montmorillonite through cetyltrimethylammonium bromide (CTAB)-assisted exfoliation and aminopropyltrimethoxysilane (AEAPTS) grafting. The results reveal that the adsorption capacity of CO_2 reached 1.8 mmol/g at the CO_2 concentration of 15vol% and adsorption temperature of 95°C. However, amino silane grafting exhibited a lower loading amount than organic amine leaching, resulting in a low adsorption capacity. Table 4 presents the CO_2 adsorption capacity of amino silane-grafted natural minerals.

When amino silane is used to modify different minerals, especially fibrous clay minerals, without pretreatment (such as sepiolite and palygorskite), it poses other modification effects that may not necessarily increase the adsorption capacity for CO_2. Such a condition is due to the likelihood of amino silane blocking the nanopore structure within minerals during grafting, which is not conducive to CO_2 diffusion [56–57]. Cecilia *et al.* [57] investigated the effect of APTES-

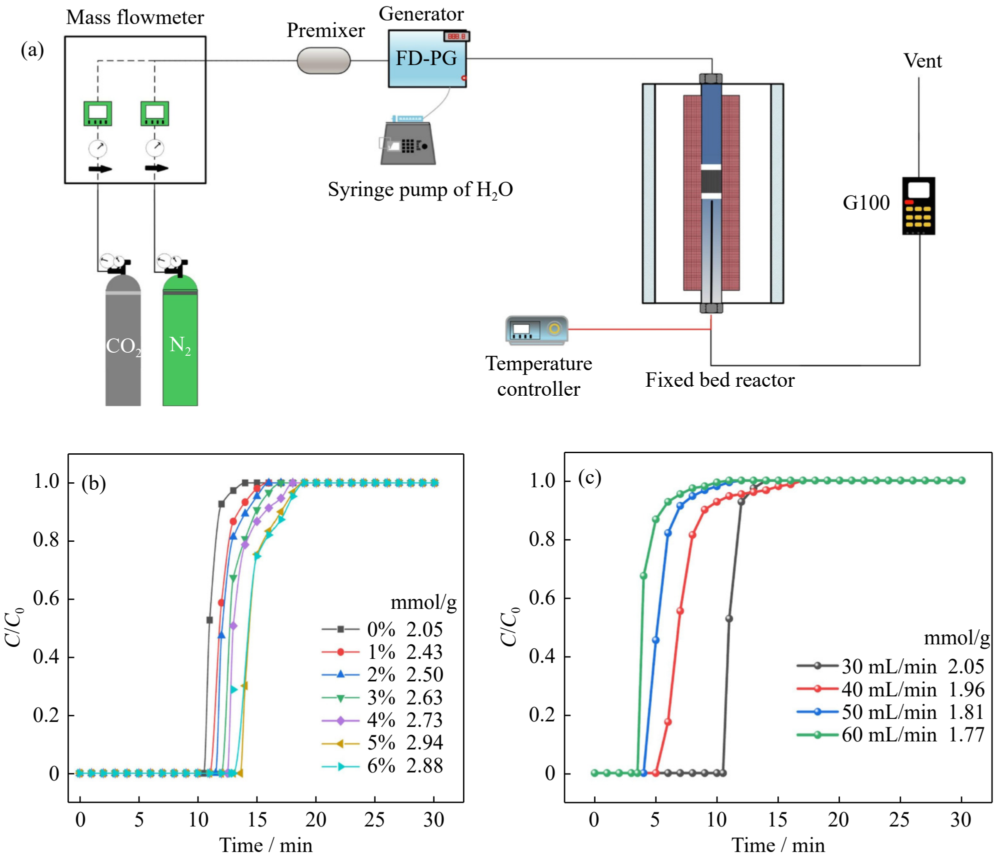

Fig. 7. (a) Composition diagram of CO_2 fixed-bed reaction system; CO_2 breakthrough adsorption curve and adsorption capacity at (b) various flow rates (C_0 and C are the initial concentration and outlet concentration of CO_2, vol%) and (c) different water contents [58]. Reprinted from *Sep. Purif. Technol.*, Vol. 306, H. Zhu, S.M. Li, J.F. Zhang, L.K. Zhao, and Y. Huang, A highly effective and low-cost sepiolite-based solid amine adsorbent for CO_2 capture in post-combustion, 122627, Copyright 2023, with permission from Elsevier.

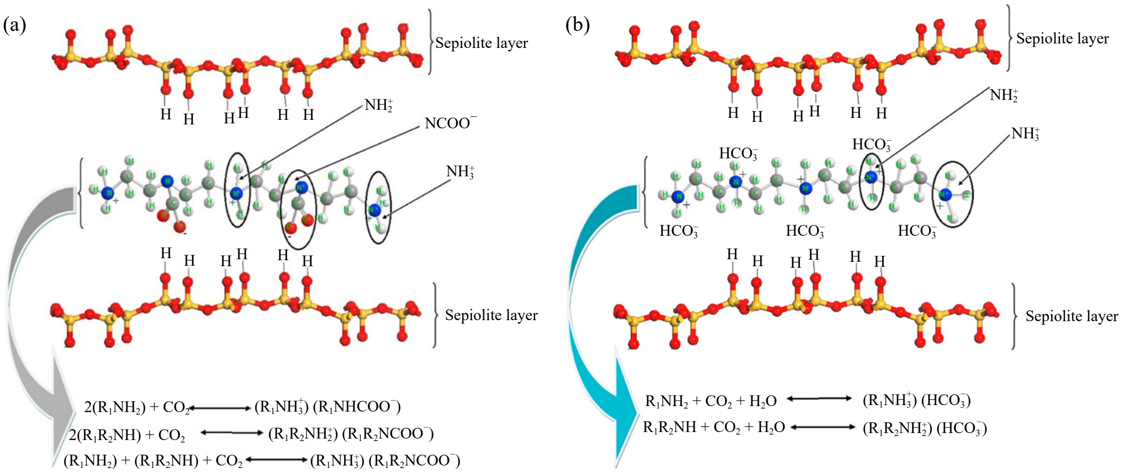

Fig. 8. CO_2 capture mechanisms of primary (R_1–NH_2) and secondary (R_1–NH–R_2) amines (a) anhydrous and (b) underwater conditions [78]. Reprinted from *Nano Energy*, Vol. 11, M. Irani, M.H. Fan, H. Ismail, A. Tuwati, B. Dutcher, and A.G. Russell, Modified nanosepiolite as an inexpensive support of tetraethylenepentamine for CO_2 sorption, 235-246, Copyright 2015, with permission from Elsevier.

grafted acid-modified sepiolite and palygorskite on CO_2 adsorption performance. Studies have shown that after APTES grafting, the pore structure of sepiolite and palygorskite is blocked, which is not beneficial to the physical adsorption of CO_2 and thus results in a decreased CO_2 adsorption performance.

To further enhance the adsorption capacity of amino silane-grafted minerals and fully take advantage of the natural properties of minerals, some scholars have proposed combining minerals with other porous materials to prepare porous

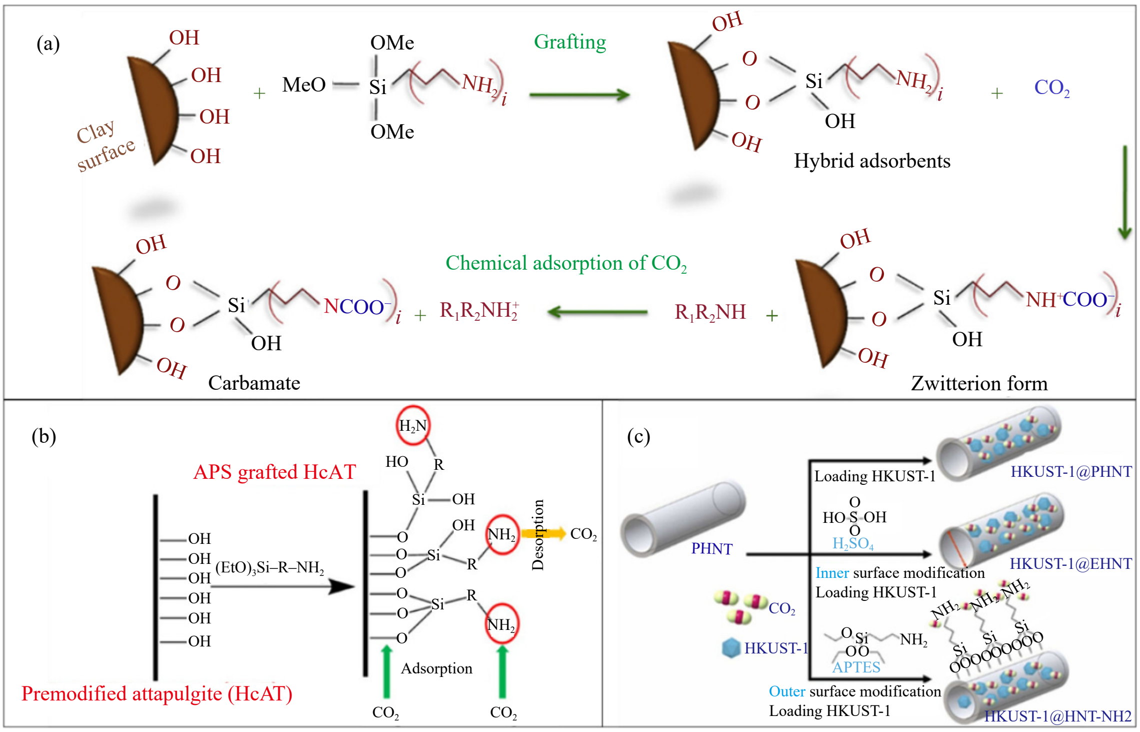

Fig. 9. (a) Schematic of amino silane-grafted clay minerals [54]; (b) schematic of AEAPTS-grafted attapulgite [84]; (c) (3-aminopropyl) triethoxysilane (APTES)-grafted HKUST-1 (MOF)-loaded halloysite used in the preparation of composite adsorption materials [85]. (a) Reprinted from *Appl. Clay Sci.*, Vol. 180, N. Horri, E.S. Sanz-Pérez, A. Arencibia, R. Sanz, N. Frini-Srasra, and E. Srasra, Amine grafting of acid-activated bentonite for carbon dioxide capture, 105195, Copyright 2019, with permission from Elsevier. (b) Reprinted with permission from S. Chen, B. Jia, Y. Peng, *et al.*, *Ind. Eng. Chem. Res.*, vol. 360, 17150-17161 (2021) [84]. Copyright 2021 American Chemical Society. (c) Reprinted from *Colloids Surf. A*, Vol. 651, S. Park, J. Ryu, H.Y. Cho, and D. Sohn, Halloysite nanotubes loaded with HKUST-1 for CO_2 adsorption, 129750, Copyright 2022, with permission from Elsevier.

Table 4. CO_2 adsorption capacity of amino silane-grafted natural minerals

Support	Pretreatment	Modifier	Adsorption conditions			CO_2 uptake / ($mmol \cdot g^{-1}$)	Ref.
			Temperature / °C	Atmosphere	Pressure / MPa		
Halloysite	Microwave-assisted acid treatment	APTES	25	CO_2	0.1	0.11	[52]
Palygorskite	Hydration treatment	APTES DT	45	CO_2	0.1	0.86 1.29	[56]
	Microwave-assisted acid treatment	APTES	25	CO_2	0.1	0.75	[57]
	Calcination and hydrochloric acid treatment	APTES	40	Air	0.1	1.81	[84]
Sepiolite	Hydration treatment	APTES DT	45	CO_2	0.1	0.99 1.39	[56]
	Microwave-assisted acid	APTES	25	CO_2	0.1	1.0	[57]
Montmorillonite	Hydration treatment	APTES DT	45	CO_2	0.1	0.75 1.13	[56]
	Inserted layer treatment	AEAPTS	95	15vol%CO_2 +85vol%N_2	0.1	1.80	[86]
Bentonite	Hydrochloric acid treatment	APTES	30	CO_2	0.1	0.66	[54]
	Hydration treatment	APTES DT	45	CO_2	0.1	0.98 0.73	[56]
	NaCl and CTAB treatment	APTES	25	CO_2	0.1	1.14	[80]

Note: DT represents N1-(3-trimethoxysilylpropyl) diethylenetriamine.

composite materials. Park *et al.* [85] first prepared HKUST-1 MOF@HNT composites through vacuum loading and solvothermal reaction and HKUST-1@HNT composites via internal corrosion and external surface amination using sulfuric acid and APTES (Fig. 9(c)). Studies have shown that HNT acts as a nanocarrier, the internal HKUST-1 improves gas adsorption capacity, and the grafting of amino silane on the HNT outer surface promotes CO_2 adsorption selectivity.

2.2.4. IL modification

Traditional organic amine leaching solid adsorbents suffer from insufficient stability during cyclic regeneration. On the one hand, they are prone to aging during cycling because of the low boiling point of organic amines. On the other hand, organic amines exhibit a weak binding capability toward the carrier surface, which may cause the detachment of amines during the adsorption process [87]. Although amino silane-grafted solid adsorbents are more stable than organic amine-impregnated solid adsorbents, the adsorption capacity of modified solid adsorbents is limited. Therefore, new solid adsorption materials must be explored.

ILs have attracted extensive attention due to their high capacity, good chemical and thermal stability, easy separation, and recyclability. To improve the utilization efficiency of ILs, reduce costs, and improve the cycle performance of materials, Chen *et al.* [87] used an ion-exchange method to synthesize an amine polycarboxylate IL $[P_{4442}]_2[IDA]$ with multiple adsorption sites for the modification of attapulgite and synthesized a new solid adsorption material for CO_2 capture. An adsorption capacity of 1.531 mmol/g was observed at the adsorption temperature of 30°C and $[P_{4442}]_2[IDA]$ loading of 30wt%. After 10 cycles, the adsorption capacity of the solid material for CO_2 was reduced slightly, which indicates an excellent recycling performance. Hu and Zhang [88] prepared adsorption materials using halloysite as a nanomineral adsorbent matrix and acetate–ethanolamine solution as a modifier. The results show that the adsorption efficiency of halloysite modified by IL can reach 23.33% at room temperature and atmospheric pressure, and such a value is considerably higher than that of CO_2 adsorption after calcination.

2.2.5. Pillared or metal-doped modification

Pillared interlayer clay (PILC) is a two-dimensional molecular sieve porous material known for its large specific surface area, uniform pore structure, and large interlayer spacing. This material shows promise as a catalyst and adsorption material [89–90]. In addition, as CO_2 is an acidic gas, some alkaline metals can be doped into minerals. Alkaline metals contain active sites that can interact with CO_2, which enhances the adsorption capacity of pillared clays for CO_2 [91–92]. Wang *et al.* [22] explored the effects of Al_2O_3, ZrO_2, and TiO_2–SiO_2 pillared montmorillonites on the CO_2 adsorption performance. The CO_2 adsorption performance of different pillared montmorillonites increased with the increase in pore volume and specific surface area. The TiO_2–SiO_2 pillared montmorillonite exhibited the largest specific surface area and pore volume and the best CO_2 adsorption capacity of 1.18 mmol/g at 273 K and 1 atm. Wu *et al.* [92] studied the effect of alkali metal (Li, Na, K, and Cs) doping on the CO_2 adsorption performance of Al-pillared montmorillonite. In the preparation of alkali metal composite materials, the main method involved the addition of aluminum pillared montmorillonite to metal nitrates and pretreatment under ultrasonic radiation at 60°C. Then, calcination of the dried sample in air was conducted at 400°C for 12 h to obtain the composite material. Studies have shown that aluminum pillaring changes the specific surface area of montmorillonite and enhances its physical adsorption performance. Meanwhile, alkali metal doping mainly increased the alkalinity of samples and improved their chemical adsorption performance. The CO_2 adsorption capacities of all samples had the following order 5wt% Cs/Al-PILC > 5wt% K/Al-PILC > 5wt% Na/Al-PILC > 5wt% Li/Al-PILC > Al-PILC > montmorillonite. The increased adsorption capacity of 5Cs/Al-PILC samples for CO_2 was observed from 1.821 mmol/g before modification to 2.325 mmol/g, and the samples doped with alkali metals exhibited an excellent cycling performance (Fig. 10).

2.2.6. Bifunctional modification of impregnation and grafting

To further improve the capture efficiency of solid adsorbents for CO_2, Sanz *et al.* [93] applied a dual-functional method that combines impregnation and grafting to modify silica to simultaneously obtain amino groups with high nitrogen insertion and high mobility. The results show that the CO_2 adsorption rate of the bifunctionalized sample was increased by approximately 10%–20% compared with that of the impregnated sample. Therefore, some scholars have proposed the use of bifunctional methods for the modification of minerals [56–57,81]. Gómez-Pozuelo *et al.* [56] pregrafted 3-aminop-

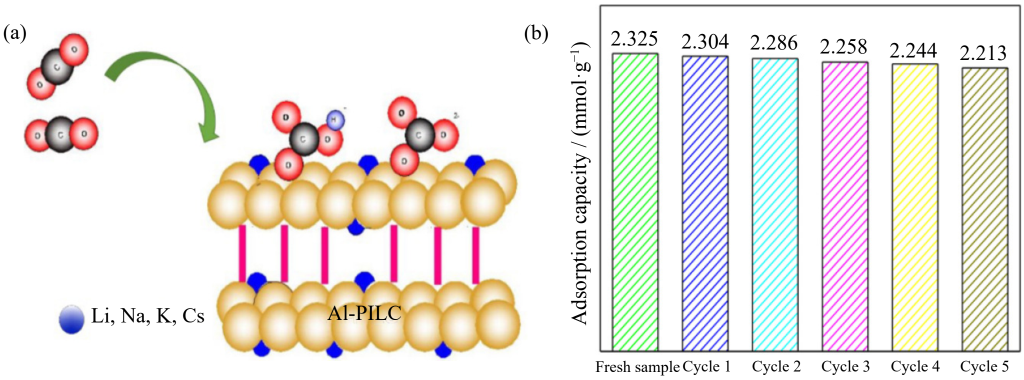

Fig. 10. (a) Adsorption of CO_2 on Al-pillared montmorillonite doped with alkali metals (Li, Na, K, and Cs); (b) regeneration experiments of the 5Cs/Al-PILC sample [92]. Reprinted from *J. Solid State Chem.*, Vol. 291, K. Wu, Q. Ye, R.P. Wu, and H.X. Dai, Alkali metal-promoted aluminum-pillared montmorillonites: High-performance CO_2 adsorbents, 121585, Copyright 2020, with permission from Elsevier.

ropyl-trimethoxysilane or diethylenetriamine-propyl-trimethoxysilane on montmorillonite, sepiolite, bentonite, and other minerals and achieved bifunctional modification by PEI impregnation (Fig. 11). The results reveal that the CO_2 adsorption capacity of bifunctional samples did not improve compared with that of samples prepared via a single impregnation or grafting method, but the value is close to that of nonfunctionalized montmorillonite. The main reason for this phenomenon is the likelihood of double-functionalized samples blocking the structural pores in minerals, which is not advantageous to CO_2 diffusion, given the limitation of the porous structure of montmorillonite and sepiolite. To solve the clogging problem of adsorbents after dual functionalization, Cecilia *et al.* [57] treated acid-leached sepiolite by grafting it with APTES (AP) and dipping in PEI; they also proposed that the increased adsorption temperature benefited the rearrangement of the amine-rich polymer and CO_2 diffusion; as a result, the amine sites were more fully in contact with CO_2, thereby improving the CO_2 adsorption capacity of the composite.

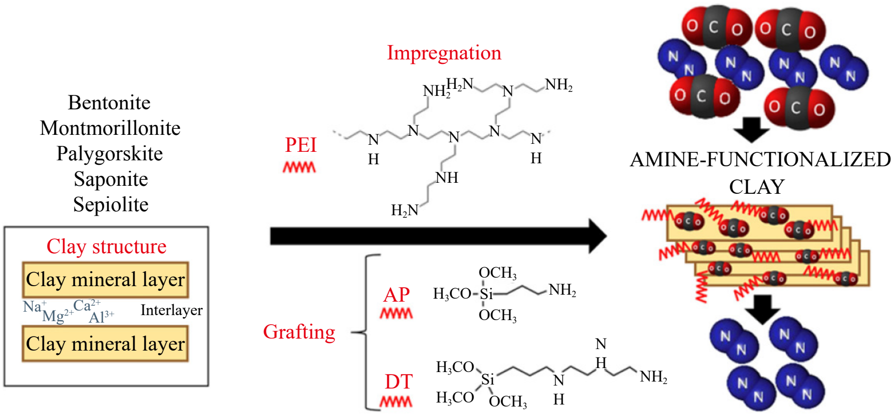

Fig. 11. Bifunctionally modified clay minerals used to prepare CO_2 adsorption materials [56]. Reprinted from *Microporous Mesoporous Mater.*, Vol. 282, G. Gómez-Pozuelo, E.S. Sanz-Pérez, A. Arencibia, P. Pizarro, R. Sanz, and D.P. Serrano, CO_2 adsorption on amine-functionalized clays, 38-47, Copyright 2019, with permission from Elsevier.

3. CO_2 mineralization by natural minerals

CO_2 mineralization mimics the weathering process of Ca/Mg silicate minerals; this phenomenon was first proposed by Seifritz and can be expressed by the following general Eq. (1) [94]. Mineralization involves the use of natural minerals, including forsterite (Mg_2SiO_4), serpentine [$Mg_3Si_2O(OH)_4$], wollastonite ($CaSiO_3$), etc. [95–96]. These natural minerals are known for their abundant reserves, easy access, and stable products after mineralization [97]. Based on different reaction processes, CO_2 mineralization can be divided into direct and indirect mineralization [20]. Direct mineralization refers to the mineralization of minerals via high-temperature and high-pressure operations under dry or wet conditions. Although the process is simple and uses fewer chemical reagents, it features high-temperature and high-pressure energy consumption, and directly obtaining high-value-added products is difficult, resulting in poor economic benefits. Therefore, some researchers have proposed indirect mineralization, in which minerals are first treated using acid, alkali, molten salt, ammonium salt, and other media to extract calcium and magnesium ions and then carbonated under certain conditions. Indirect mineralization has less harsh reaction conditions compraed with direct mineralization, and the obtained mineralized products are relatively pure and have certain economic value.

$$\begin{aligned}&(\mathrm{Ca,Mg})_x\mathrm{Si}_y\mathrm{O}_{x+2y}\cdot z\mathrm{H_2O}\,(\mathrm{s})+x\mathrm{CO_2}\,(\mathrm{g})\rightarrow\\&\quad x(\mathrm{Ca,Mg})\mathrm{CO_3}\,(\mathrm{s})+y\mathrm{SiO_2}\,(\mathrm{s})+z\mathrm{H_2O}\,(\mathrm{l/g})\end{aligned}\qquad(1)$$

3.1. Direct mineralization of natural minerals

Based on different reaction modes between minerals and CO_2, direct mineralization can be divided into dry and wet carbonation [44]. Dry carbonation refers to the direct reaction of CO_2 with minerals at appropriate temperature and pressure. Wet carbonation involves the reaction of CO_2 with minerals in an aqueous suspension [98], in which CO_2 reacts with water to form bicarbonate and protons. Then, the protons dissolve metal ions, which can react with sodium bicarbonate to form carbonate precipitates in minerals.

Lackner *et al.* [95,97] first proposed the gas–solid carbonation of CO_2. Through thermodynamic calculations, they showed that the gas–solid reaction of serpentine, olivine, and basalt with CO_2 is an exothermic process. It can spontaneously react in nature, but the reaction rate is usually low. Wet carbonation was first proposed by O'Connor *et al.* [98]. Fig. 12 shows the process flow, and Eqs. (2)–(4) provide the reaction path; that is, CO_2 dissolves in water to form carbonic acid. Then, the ore gradually dissolves and precipitates carbonate under the action of carbonic acid.

$$\mathrm{CO_2+H_2O\rightarrow H_2CO_3\rightarrow H^++HCO_3^-}\qquad(2)$$

$$\mathrm{Mg_2SiO_4+4H^+\rightarrow 2Mg^{2+}+H_4SiO_4(SiO_2+2H_2O)}\qquad(3)$$

$$\mathrm{Mg^{2+}+HCO_3^-\rightarrow MgCO_3+H^+}\qquad(4)$$

Huijgen *et al.* [99] reported the mechanism of direct mineralization of wollastonite in aqueous solutions. According to studies, throughout the carbonation process, factors such as reaction temperature, stirring speed, and liquid–solid ratio

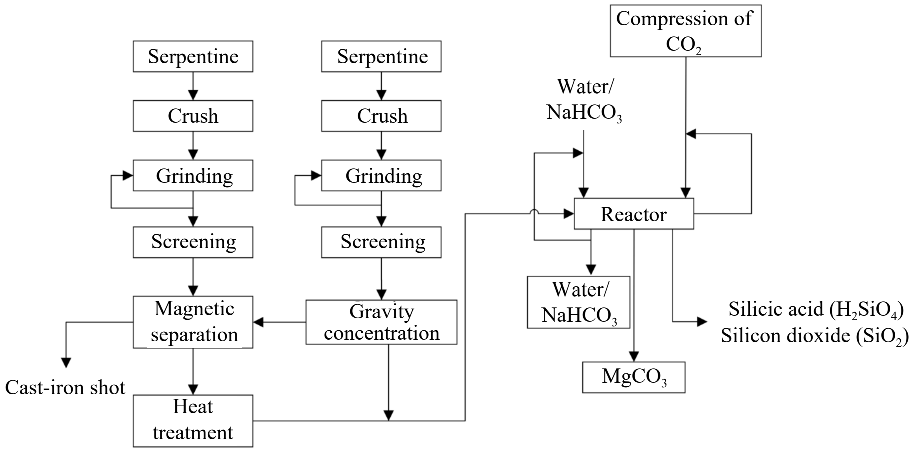

Fig. 12. Schematic of the wet carbonation process [98]. Adapted by permission from Springer Nature: *Min. Metall. Explor.*, Carbon dioxide sequestration by direct mineral carbonation: Process mineralogy of feed and products, W.K. O'Connor, D.C. Dahlin, G.E. Rush, C.L. Dahlin, and W.K. Collins, Copyright 2002.

considerably influence the mineralization process of wollastonite. Reaction temperature affects the leaching of calcium and magnesium ions and nucleation efficiency of carbonates. At lower than optimal temperatures, the dissolution of calcium and magnesium ions on the outer surface during the mineralization process leaves a dense outer layer of SiO_2. This condition affects the outward diffusion of calcium and magnesium ions from within the mineral and leads to leaching difficulties, whereas at high reaction temperatures, it influences the nucleation and growth of carbonates due to the lower activity of the generated carbonates. Stirring speed affects the leaching efficiency of calcium and magnesium ions, with the appropriate stirring speed being conducive to the carbonation of minerals. The liquid–solid ratio influences the thermal balance of the reaction process, which results in changes in the carbonation efficiency of minerals. At extremely low liquid–solid ratios, the viscosity of the reaction system increases, and problems such as difficult pumping and stirring occur, which drastically reduce the conversion efficiency. Meanwhile, an extremely high liquid–solid ratio leads to a reduced processing capacity of the reaction, which is not conducive to the industrialization of applications. In addition, improvement of the reaction rate of wet carbonation can be attained through pressure control in the reaction process, the addition of additives (such as $NaHCO_3$ and NaCl [100–101]), ore treatment (such as heating activation [102–103], mechanical grinding [104–105]), and removal of the formed SiO_2 inert surface layer. Table 5 shows the findings of the comparison of typical process parameters during the direct mineralization of CO_2 by natural silicate minerals.

However, the entire process of direct mineralization still faces problems, such as harsh reaction conditions, high equipment requirements, high energy consumption during pretreatment, and low economic value of carbonization products. Therefore, the focus of the research on CO_2 mineralization has gradually shifted to indirect mineralization.

3.2. Indirect mineralization of natural minerals

In indirect mineralization, the active ingredients (such as calcium and magnesium ions) in mineral raw materials are

Table 5. Comparison of typical process parameters during the direct mineralization of CO_2 by natural silicate minerals

Mineral type	Particle size / μm	Chemical additives	Reaction conditions					Mineralization rate / %	Ref.
			Liquid–solid ratio	Temperature / °C	Pressure / MPa	Time / h	Stirring speed / (r·min^{-1})		
Wollastonite	37–44	1 M $NaHCO_3$	9 g/g	110	8.6	6	—	90	[100]
Wollastonite	<38	—	5 kg/kg	200	2.0	0.25	500	75	[106]
Olivine	<37	1 M NaCl, 0.5 M $NaHCO_3$	5.6 g/g	185	11.5	6	—	84	[98]
Olivine	<38	1 M NaCl, 0.64 M $NaHCO_3$	2.33 g/g	185	15	1	—	49.5	[107]
Olivine	<10	0.75 M NaCl, 0.5 M $NaHCO_3$	5 mL/g	190	10	4	1500	100	[108]
Olivine	<38	1 M NaCl, 0.64 M $NaHCO_3$	9 mL/g	185	6.5	6	1420	84.4	[109]
Serpentine	<37	1 M NaCl, 0.64 M $NaHCO_3$	5.6 mL/g	155	18.5	0.5	2000	78	[98]
Serpentine	<75	1 M NaCl, 0.64 M $NaHCO_3$	2.33 g/g	155	11.5	1	—	73.5	[107]

first dissolved in the medium and then carbonated to form carbonates. Media screening is a key step in indirect mineralization. The reaction medium used must have two characteristics: (1) benefiting the leaching of calcium and magnesium ions; (2) easily recycled in the carbonation reaction process. The common media used in indirect mineralization mainly include hydrochloric acid, acetic acid, sodium hydroxide, molten salt, etc. Table 6 shows the findings of the comparison of typical process parameters in the indirect mineralization of CO_2 by natural silicate minerals.

3.2.1. Acid extraction

Regarding reaction mediums, ores can be quickly dissolved in hydrochloric acid solution to form magnesium chloride, calcium chloride, and silica. This hydrochloric acid extraction process was developed in the 1940s and 1950s and was mainly used to extract magnesium from serpentine [115]. The reaction mechanisms are shown in Eqs. (5)–(8) [116]. The process mainly includes four steps: dissolution of serpentine by hydrochloric acid to form magnesium chloride, decomposition of magnesium chloride into Mg(OH)Cl at 150°C in water and excess hydrochloric acid, decomposition of Mg(OH)Cl into magnesium hydroxide and magnesium chloride, and formation of magnesium carbonate in CO_2 atmosphere. The magnesium chloride and hydrochloric acid produced in this process can be recycled. Despite the effectiveness of this method, it still presents shortcomings, such as high energy consumption and strong equipment corrosion in the hydrochloric acid regeneration process, which limit its industrial application.

$$\mathrm{Mg_3Si_2O_5(OH)_4\,(s) + 6HCl\,(aq) + H_2O \rightarrow 3MgCl_2 \cdot 6H_2O\,(aq) + 2SiO_2\,(s)} \tag{5}$$

$$\mathrm{MgCl_2 \cdot 6H_2O\,(aq) \rightarrow MgCl\,(OH)\,(aq) + HCl\,(aq) + 5H_2O} \tag{6}$$

$$\mathrm{2MgCl\,(OH)\,(aq) \rightarrow Mg(OH)_2\,(s) + MgCl_2(aq/s)} \tag{7}$$

$$\mathrm{Mg(OH)_2\,(s) + CO_2\,(g) \rightarrow MgCO_3\,(s) + H_2O} \tag{8}$$

In addition to hydrochloric acid extraction, other acids have been studied as mediators in the indirect mineralization process. Teir *et al.* [117] investigated the dissolution of natural serpentine in inorganic acids (HCl, H_2SO_4, HNO_3, etc.), organic acids (HCOOH, CH_3COOH, etc.), ammonium salt solutions ($(NH_4)_2SO_4$, NH_4Cl, NH_4Cl, etc.), and alkali solutions (NaOH, KOH, NH_3, etc.). The results reveal that all the tested acids can extract 3%–26% magnesium and 2%–16% iron from serpentine within 1 h at room temperature at 1–4 M acid concentration, with H_2SO_4 showing the highest extraction efficiency. Ammonium salt solution is the only selective solution used in magnesium extraction. However, its extraction rate is considerably lower than that of the acid used, and the alkaline solution fails to dissolve any measurable magnesium and iron. Teir *et al.* [110] used 2 mol/L H_2SO_4 to leach serpentine at 70°C. Almost all Mg can be extracted to the leaching solution, and the reaction equations are shown in Eqs. (9)–(11). In addition, approximately 65% of Fe and 3% of Si were extracted, and NaOH was used to remove Fe from the leaching solution for carbonation reaction. The carbonation rate of Mg can reach 94%. However, this process consumes extremely strong acids and alkalis, and the whole mineralization process is uneconomical.

$$\mathrm{Mg_3Si_2O_5(OH)_4\,(s) + 3H_2SO_4\,(aq) \rightarrow 3MgSO_4\,(aq) + 2SiO_2\,(s) + 5H_2O\,(l)} \tag{9}$$

$$\mathrm{FeO\,(s) + H_2SO_4\,(aq) \rightarrow FeSO_4\,(aq) + H_2O\,(l)} \tag{10}$$

$$\mathrm{MgSO_4\,(aq) + 2NaOH\,(aq) + CO_2\,(g) \rightarrow MgCO_3\,(s) + H_2O\,(l) + Na_2SO_4\,(aq)} \tag{11}$$

O'Connor *et al.* [118] proposed that weak acids can be used instead of strong ones to lower energy consumption, and the recovery of media is relatively easy. The main reaction processes are shown in Eqs. (12)–(13).

$$\mathrm{CaSiO_3\,(s) + 2HAc\,(l) \rightarrow Ca^{2+}\,(aq) + 2Ac^-\,(aq) + H_2O\,(l) + SiO_2\,(s)} \tag{12}$$

$$\mathrm{Ca^{2+}\,(aq) + 2Ac^-\,(aq) + CO_2\,(g) + H_2O\,(l) \rightarrow CaCO_3\,(s) + 2HAc\,(l)} \tag{13}$$

Bao *et al.* [114] studied the carbon fixation process through the addition of tributyl phosphate (TBP) and magnesium acetate to acetic acid as the circulating medium (Fig. 13). The reaction processes are shown in Eqs. (14)–(19). This carbon-fixation process involves CO_2 diffusion, dissolution, and ionization, calcium carbonate precipitation, and TBP acetic acid extraction, which can realize the recycling of acetic acid. However, the additives have the disadvantages of high energy consumption and complex processes during recovery, which increase the economic cost and additional carbon emissions. Despite the effectiveness of indirect mineral carbon sequestration via acid extraction, the cost is usually high. Thus, scholars should focus on explor-

Table 6. Comparison of typical process parameters during indirect mineralization of CO_2 by natural silicate minerals

Mineral type	Particle size / μm	Chemical additives	Reaction conditions					Mineralization rate / %	Ref.
			Liquid–solid ratio	Temperature / °C	Pressure / MPa	Time / h	Stirring speed / (r·min^{-1})		
Serpentine	<500	2 M H_2SO_4, NaOH	10 mL/g	70	0.1	1	650	94	[110]
Lizardite	<150	2 M HCl, NH_3	13.51 mL/g	90	0.1	2	600–700	80	[111]
Serpentine	75–150	1.4 M NH_4HSO_4, NH_3	20 mL/g	100	0.1	1	800	86	[112]
Serpentine	125–212	$(NH_4)_2SO_4$	—	400	0.1	1	—	78	[113]
Wollastonite	—	1.52 M CH_3COOH, TBP	—	80	4.0	1	500	50	[114]

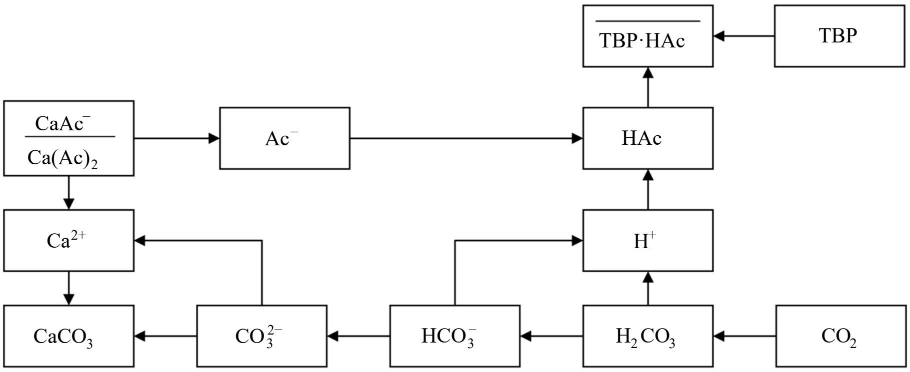

Fig. 13. Reaction scheme for enhanced carbonation via solvent extraction. W.J. Bao, H.Q. Li, and Y. Zhang, *Greenhouse Gases Sci. Technol.*, vol. 4, 785-799 (2014) [114]. Copyright Wiley-VCH Verlag GmbH & Co. KGaA. Reproduced with permission.

ing new extraction methods.

$$CO_2(g) \Longleftrightarrow CO_2(aq) \tag{14}$$

$$CO_2(aq) + H_2O(l) \Longleftrightarrow H_2CO_3(aq) \tag{15}$$

$$H_2CO_3(aq) \rightarrow 2H^+(aq) + CO_3^{2-}(aq) \tag{16}$$

$$Ca^{2+}(aq) + CO_3^{2-}(aq) \Longleftrightarrow CaCO_3(s) \tag{17}$$

$$Ac^-(aq) + H^+(aq) \Longleftrightarrow HAc(aq) \tag{18}$$

$$TBP(aq) + HAc(aq) \Longleftrightarrow TBP \cdot HAc(aq) \tag{19}$$

3.2.2. Molten salt extraction

Molten salt extraction is similar to HCl extraction, except for the use of molten salt ($MgCl_2 \cdot n(H_2O)$) instead of HCl as an extractant to reduce the energy consumption of CO_2 during mineralization [119]. With serpentine as an example, the reaction processes are shown in Eqs. (20)–(23) [120]. Although the molten salt process consumes lower energy consumption than the HCl extraction process, rock impurities react with chloride ions, which causes the loss of chloride ions, and $MgCl_2$ cannot be recovered. The complex process is difficult to operate and devoid of industrial application value.

$$\begin{aligned} &3MgCl_2 \cdot 3.5H_2O(l) + Mg_3Si_2O_5(OH)_4(s) \rightarrow \\ &\quad 6Mg(OH)Cl(l) + 9.5H_2O(l) + 2SiO_2(aq) \end{aligned} \tag{20}$$

$$\begin{aligned} &2Mg(OH)Cl(l) + nH_2O(l) \rightarrow \\ &\quad MgCl_2 \cdot nH_2O(l) + Mg(OH)_2(s) \end{aligned} \tag{21}$$

$$\begin{aligned} &MgCl_2 \cdot nH_2O(l) \rightarrow \\ &\quad MgCl_2 \cdot 3.5H_2O(l) + (n-3.5)H_2O(l) \end{aligned} \tag{22}$$

$$Mg(OH)_2(s) + CO_2(g) \rightarrow MgCO_3(s) + H_2O(g) \tag{23}$$

3.2.3. Sodium hydroxide extraction

Blencoe *et al.* [121] first proposed the use of NaOH in the extraction of Ca and Mg from metal silicate minerals to achieve mineral carbonation. With wollastonite as an example, the main reaction processes are shown in Eqs. (24)–(26). This extraction method has many problems, including (1) large energy consumption due to the long reaction time and high reaction temperature; (2) consumption of a large amount of alkali due to the high silicon content of the raw material; (3) difficulty of obtaining pure $CaCO_3$ because of challenging product separation. Thus, NaOH is not an ideal medium for mineral carbonation in indirect mineralization carbonation technology.

$$CaSiO_3(s) + NaOH(aq) \rightarrow NaCaSiO_3(OH)(s) \tag{24}$$

$$2NaOH(aq) + CO_2(aq) \rightarrow Na_2CO_3(aq) + H_2O \tag{25}$$

$$\begin{aligned} &Na_2CO_3(aq) + 3NaCaSiO_3(OH)(s) + H_2O \rightarrow \\ &\quad 4NaOH(aq) + CaCO_3(s) + NaCa_2Si_3O_8(OH)(s) \end{aligned} \tag{26}$$

3.2.4. Ammonium salt extraction

The dissolution and carbonation of minerals usually consume large amounts of acid, alkali, and other media, which are difficult to recycle during use. To overcome the above limitations, Wang and Maroto-Valer [112] used a series of ammonium salt solutions (such as $(NH_4)_2SO_4$, NH_4Cl, and NH_4HSO_4) to dissolve serpentine; NH_4HSO_4 showed the highest effectivity in the extraction from serpentine samples; a comprehensive capture-and-storage process based on mineral carbonation using recyclable ammonium salts was also proposed (Fig. 14). The process initially used NH_4HSO_4 to dissolve magnesium ions from serpentine and then adjusted the pH through the addition of ammonia for the removal of impurities in the solvent. Second, after the removal of impurities, the solution was reacted with the NH_4HCO_3 formed by NH_3 by capturing CO_2 to form the precipitated carbonate. Finally, the solution mainly contained ammonium sulfate, which can be collected through evaporation and heated to regenerate ammonia. NH_4HSO_4 and NH_3 can be recycled in this process. The results show that NH_4HSO_4 dissolved serpentine at 100°C for 3 h, and the extraction rate of Mg reached 100%. NH_4HCO_3 was reacted with Mg^{2+}, and the resulting magnesium carbonate precipitation can reach up to 96%. However, in this process, ammonium sulfate consumed a notably high thermal decomposition energy, and the heat generated by mineralization reaction and mineral dissolution was difficult to utilize, resulting in energy loss.

To fully utilize the heat of acidolysis and mineralization, the reseachers [113,122] combined the regeneration and extraction process of ammonium bisulfate and used the heat of acidolysis and mineralization to accelerate the dissolution of serpentine and thermal decomposition of ammonium sulfate (Fig. 15). For the further improvement of the economics of the mineralization process, in addition to reduced energy consumption, mineralized (e.g., calcium carbonate and magnesium carbonate) and high value-added products [113,123–124] (e.g., porous silica and metals such as Cu and Ni) can be recovered.

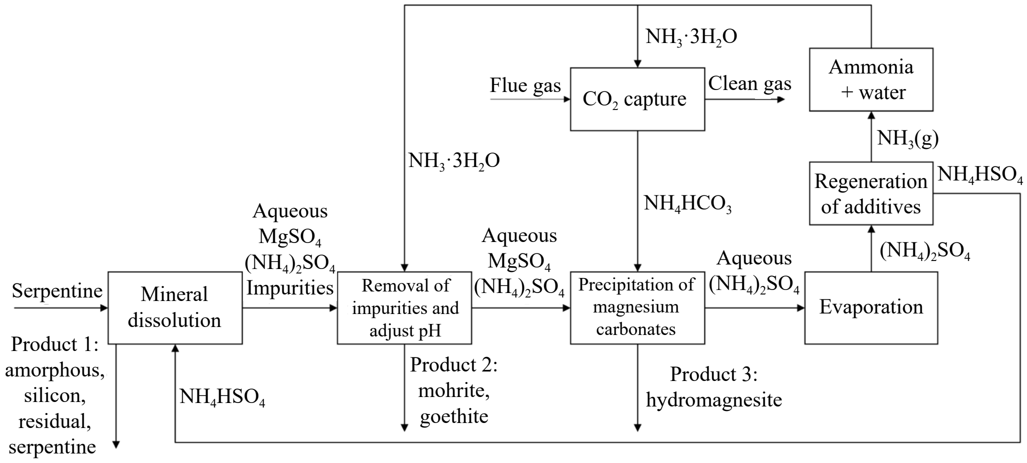

Fig. 14. Schematic process route of pH-swing CO_2 mineral sequestration with recyclable ammonium salts [112]. Reprinted from *Fuel*, Vol. 90, X.L. Wang and M.M. Maroto-Valer, Dissolution of serpentine using recyclable ammonium salts for CO_2 mineral carbonation, 1229-1237, Copyright 2011, with permission from Elsevier.

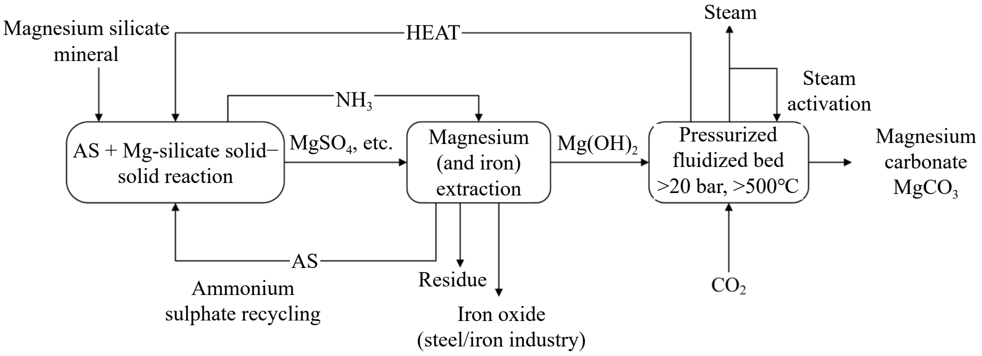

Fig. 15. CO_2 mineralization process using recyclable $(NH_4)_2SO_4$ as an additive (AS: ammonium sulphate) [113]. Reprinted from *Energy*, Vol. 41, J. Fagerlund, E. Nduagu, I. Romão, and R. Zevenhoven, CO_2 fixation using magnesium silicate minerals part 1: Process description and performance, 184-191, Copyright 2012, with permission from Elsevier.

4. Conclusions

Excessive CO_2 emissions cause global warming, which substantially influences social, economic, and human production and development. In this context, the technology of CO_2 capture and storage, which is deemed a highly effective method to mitigate CO_2 emissions, has caught the interest of numerous scholars. This paper reviewed the progress of the research on CO_2 capture and mineralization by natural minerals, with a focus on various methods that enhance CO_2 capture and mineralization by natural minerals. Despite the considerable number of research advances, CO_2 capture and mineralization by natural minerals still face many difficulties and challenges.

In terms of CO_2 capture by natural minerals, the capability of adsorbents to capture CO_2 is affected by the type of minerals, pretreatment methods, modifiers and modification conditions, adsorption conditions (concentration and flow rate of CO_2, adsorption temperature and pressure, water content, etc.), and other factors. Meanwhile, pretreatment and modification methods directly affect the performance of solid adsorbents. Therefore, in the selection of pretreatment and modification methods, the inherent properties of minerals must be thoroughly considered, and the potential synergy between different modification techniques must be assessed. In addition, future research on CO_2 capture by natural minerals will focus on the exploration of composite materials with high specific surface area and numerous active sites. Adsorption conditions affect the capacity of adsorbents to capture CO_2. In determining adsorption conditions, simulation of the state of mixed gas during actual production is required to evaluate the adsorption capacity of solid adsorbents, and suitable mineral-based solid adsorbents must be prepared for different gas environments.

In terms of CO_2 mineralization by natural minerals, indirect mineralization is milder than direct mineralization and does not require high-concentration and high-pressure CO_2 as raw materials. The acquired mineralized products have high purity and possess economic value. However, several issues, including additional energy consumption, large consumption of media, and difficulty in utilizing heat generated by mineralization reactions and mineral dissolution, remain to be addressed. Therefore, future research on CO_2 mineralization by natural minerals should focus on the development of new mineralization technologies (such as the combination of CO_2 adsorption and mineralization) to reduce energy consumption during indirect mineralization, recycling of media, and full usage of high-value-added products.

Given strict carbon emission and neutral targets, it is necessary to promote the industrialization of CO_2 capture and mineralization. However, the current research on natural mineral CO_2 capture and mineralization mainly focuses on the laboratory stage. Therefore, practical applications should be simulated at a later stage, and related research should be accelerated from the laboratory stage to the pilot scale-up stage. In addition, the economic cost analysis of CO_2 capture and mineralization is important. The development and industrialization of CO_2 capture and mineralization technology can be further promoted through the establishment of a cost assessment system related to CO_2 capture and mineralization.

Acknowledgement

This work was financially supported by the Beijing Natural Science Foundation, China (No. 2242055).

Conflict of Interest

The authors declare that they have no conflicts of interest.

References

[1] B. Bereiter, S. Eggleston, J. Schmitt, *et al.*, Revision of the EPICA Dome C CO_2 record from 800 to 600 kyr before present, *Geophys. Res. Lett.*, 42(2015), No. 2, p. 542.

[2] M.S.B. Reddy, D. Ponnamma, K.K. Sadasivuni, B. Kumar, and A.M. Abdullah, Carbon dioxide adsorption based on porous materials, *RSC Adv.*, 11(2021), No. 21, p. 12658.

[3] M.R. Raupach, G. Marland, P. Ciais, *et al.*, Global and regional drivers of accelerating CO_2 emissions, *Proc. Natl. Acad. Sci. USA*, 104(2007), No. 24, p. 10288.

[4] J. Blamey, E.J. Anthony, J. Wang, and P.S. Fennell, The calcium looping cycle for large-scale CO_2 capture, *Prog. Energy Combust. Sci.*, 36(2010), No. 2, p. 260.

[5] J.M. Pandolfi, S.R. Connolly, D.J. Marshall, and A.L. Cohen, Projecting coral reef futures under global warming and ocean acidification, *Science*, 333(2011), No. 6041, p. 418.

[6] M.J. Hu, M.Z. Yin, L.W. Hu, P.J. Liu, S. Wang, and J.B. Ge, High-value utilization of CO_2 to synthesize sulfur-doped carbon nanofibers with excellent capacitive performance, *Int. J. Miner. Metall. Mater.*, 27(2020), No. 12, p. 1666.

[7] M.Q. Cao, K. Liu, H.M. Zhou, *et al.*, Hierarchical TiO_2 nanorods with a highly active surface for photocatalytic CO_2 reduction, *J. Cent. South Univ.*, 26(2019), No. 6, p. 1503.

[8] H.Q. Yang, Z.H. Xu, M.H. Fan, *et al.*, Progress in carbon dioxide separation and capture: A review, *J. Environ. Sci.*, 20(2008), No. 1, p. 14.

[9] K. Menyah and Y. Wolde-Rufael, CO_2 emissions, nuclear energy, renewable energy and economic growth in the US, *Energy Policy*, 38(2010), No. 6, p. 2911.

[10] P. Wang, X.B. Mao, and S.E. Chen, CO_2 sequestration characteristics in the cementitious material based on gangue backfilling mining method, *Int. J. Min. Sci. Technol.*, 29(2019), No. 5, p. 721.

[11] Y.C. Hu, Y.F. Guo, J. Sun, H.L. Li, and W.Q. Liu, Progress in MgO sorbents for cyclic CO_2 capture: A comprehensive review, *J. Mater. Chem. A*, 7(2019), No. 35, p. 20103.

[12] S. Paltsev, J. Morris, H. Kheshgi, and H. Herzog, Hard-to-Abate sectors: The role of industrial carbon capture and storage (CCS) in emission mitigation, *Appl. Energy*, 300(2021), art. No. 117322.

[13] Z.E. Zhang, T. Wang, M.J. Blunt, *et al.*, Advances in carbon capture, utilization and storage, *Appl. Energy*, 278(2020), art. No. 115627.

[14] L.P. Fu, Z.K. Ren, W.Z. Si, *et al.*, Research progress on CO_2 capture and utilization technology, *J. CO_2 Util.*, 66(2022), art. No. 102260.

[15] J.Y. Yan, Carbon capture and storage (CCS), *Appl. Energy*, 148(2015), p. A1.

[16] C. Hepburn, E. Adlen, J. Beddington, *et al.*, The technological and economic prospects for CO_2 utilization and removal, *Nature*, 575(2019), No. 7781, p. 87.

[17] Z.Q. Liu, J. Zheng, Y. Wang, and X. Liu, Selective reduction of carbon dioxide into amorphous carbon over activated natural magnetite, *Int. J. Miner. Metall. Mater.*, 28(2021), No. 2, p. 231.

[18] X. Lu, W.J. Tian, H. Li, X.J. Li, K. Quan, and H. Bai, Decarbonization options of the iron and steelmaking industry based on a three-dimensional analysis, *Int. J. Miner. Metall. Mater.*, 30(2023), No. 2, p. 388.

[19] P. Li, S.Y. Pan, S.L. Pei, Y.J. Lin, and P.C. Chiang, Challenges and perspectives on carbon fixation and utilization technologies: An overview, *Aerosol Air Qual. Res.*, 16(2016), No. 6, p. 1327.

[20] E.R. Bobicki, Q.X. Liu, Z.H. Xu, and H.B. Zeng, Carbon capture and storage using alkaline industrial wastes, *Prog. Energy Combust. Sci.*, 38(2012), No. 2, p. 302.

[21] M. Pera-Titus, Porous inorganic membranes for CO_2 capture: Present and prospects, *Chem. Rev.*, 114(2014), No. 2, p. 1413.

[22] K. Wang, X.L. Yan, and S. Komarneni, CO_2 adsorption by several types of pillared montmorillonite clays, *Appl. Petrochem. Res.*, 8(2018), No. 3, p. 173.

[23] T.C. Merkel, H.Q. Lin, X.T. Wei, and R. Baker, Power plant post-combustion carbon dioxide capture: An opportunity for membranes, *J. Membr. Sci.*, 359(2010), No. 1-2, p. 126.

[24] J. Godin, W.Z. Liu, S. Ren, and C.B. Xu, Advances in recovery and utilization of carbon dioxide: A brief review, *J. Environ. Chem. Eng.*, 9(2021), No. 4, art. No. 105644.

[25] H.Y. Tao, X. Qian, Y. Zhou, and H.F. Cheng, Research progress of clay minerals in carbon dioxide capture, *Renewable Sustainable Energy Rev.*, 164(2022), art. No. 112536.

[26] N. MacDowell, N. Florin, A. Buchard, *et al.*, An overview of CO_2 capture technologies, *Energy Environ. Sci.*, 3(2010), No. 11, p. 1645.

[27] R. Czarnota, E. Knapik, P. Wojnarowski, D. Janiga, and J. Stopa, Carbon dioxide separation techonlogies, *Arch. Min. Sci.*, 64(2019), No. 3, p. 487.

[28] Z.H. Ban, K.K. Lau, and M. Azmi, Physical absorption of CO_2 capture: A review, [in] L. Ismail, K.A. Azizli, T. Murugesan, S. Ganguly, and Y. Uemura, eds., *Proceedings of the International Conference on Process Engineering and Advanced Materials 2012* (*ICPEAM 2012*), Kuala Lumpur, 2012, p. 134.

[29] B.C. Liu, Y.S. Qiao, Q. Li, W.G. Jia, and T. Wang, CO_2 separation from CO_2-EOR associated gas using hollower fiber membranes: A process design and simulation study, *J. Nat. Gas Sci. Eng.*, 100(2022), art. No. 104451.

[30] Y. Han, G. Hwang, H. Kim, B.Z. Haznedaroglu, and B. Lee, Amine-impregnated millimeter-sized spherical silica foams with hierarchical mesoporous-macroporous structure for CO_2 capture, *Chem. Eng. J.*, 259(2015), p. 653.

[31] D.Y.C. Leung, G. Caramanna, and M.M. Maroto-Valer, An overview of current status of carbon dioxide capture and storage technologies, *Renewable Sustainable Energy Rev.*, 39(2014), p. 426.

[32] J.Y. Bae, CO_2 capture by amine-functionalized mesoporous hollow silica, *J. Nanosci. Nanotechnol.*, 17(2017), No. 10, p.

7418.

[33] W. Zhang, Y.S. Bao, and A. Bao, Preparation of nitrogen-doped hierarchical porous carbon materials by a template-free method and application to CO_2 capture, *J. Environ. Chem. Eng.*, 8(2020), No. 3, art. No. 103732.

[34] T. Du, L.Y. Liu, P. Xiao, S. Che, and H.M. Wang, Preparation of zeolite NaA for CO_2 capture from nickel laterite residue, *Int. J. Miner. Metall. Mater.*, 21(2014), No. 8, p. 820.

[35] Z.C. Gao, L.Q. Li, H.L. Li, R.F. Chen, S. Wang, and Y.G. Wang, A hybrid zeolitic imidazolate framework Co-IM-mIM membrane for gas separation, *J. Cent. South Univ.*, 24(2017), No. 8, p. 1727.

[36] S.P. Wang, S.L. Yan, X.B. Ma, and J.L. Gong, Recent advances in capture of carbon dioxide using alkali-metal-based oxides, *Energy Environ. Sci.*, 4(2011), No. 10, p. 3805.

[37] F.O. Ochedi, Y.X. Liu, and Y.G. Adewuyi, State-of-the-art review on capture of CO_2 using adsorbents prepared from waste materials, *Process. Saf. Environ. Prot.*, 139(2020), p. 1.

[38] F. Fang, Z.S. Li, and N.S. Cai, CO_2 capture from flue gases using a fluidized bed reactor with limestone, *Korean J. Chem. Eng.*, 26(2009), No. 5, p. 1414.

[39] J.I. Ida, R.T. Xiong, and Y.S. Lin, Synthesis and CO_2 sorption properties of pure and modified lithium zirconate, *Sep. Purif. Technol.*, 36(2004), No. 1, p. 41.

[40] N. Chouikhi, J.A. Cecilia, E. Vilarrasa-García, *et al.*, CO_2 adsorption of materials synthesized from clay minerals: A review, *Minerals*, 9(2019), No. 9, art. No. 514.

[41] F.M. Orr, Carbon capture, utilization, and storage: An update, *SPE J.*, 23(2018), No. 6, p. 2444.

[42] W.Z. Liu, L.M. Teng, S. Rohani, *et al.*, CO_2 mineral carbonation using industrial solid wastes: A review of recent developments, *Chem. Eng. J.*, 416(2021), art. No. 129093.

[43] S. Park, CO_2 reduction-conversion to precipitates and morphological control through the application of the mineral carbonation mechanism, *Energy*, 153(2018), p. 413.

[44] M.Y. He, W.Z. Liu, Q.C. Liu, and Z.F. Qin, Research progress in CO_2 mineral sequestration technology, *Chem. Ind. Eng. Prog.*, 41(2022), No. 4, p. 1825.

[45] B. Wang, Z.H. Pan, H.G. Cheng, Z.E. Zhang, and F.Q. Cheng, A review of carbon dioxide sequestration by mineral carbonation of industrial byproduct gypsum, *J. Cleaner Prod.*, 302(2021), art. No. 126930.

[46] H.P. Xie, H.R. Yue, J.H. Zhu, *et al.*, Scientific and engineering progress in CO_2 mineralization using industrial waste and natural minerals, *Engineering*, 1(2015), No. 1, p. 150.

[47] Y.H. Chen and D.L. Lu, CO_2 capture by kaolinite and its adsorption mechanism, *Appl. Clay Sci.*, 104(2015), p. 221.

[48] Q.H. Liu, J.L. Jiang, F. Zhang, *et al.*, CO_2 fixation mechanism of kaolin treated with organic amines at varied temperatures and pressure, *Appl. Clay Sci.*, 228(2022), art. No. 106638.

[49] Y.H. Chen and D.L. Lu, Amine modification on kaolinites to enhance CO_2 adsorption, *J. Colloid Interface Sci.*, 436(2014), p. 47.

[50] X.D. Du, D.D. Pang, Y. Zhao, Z.K. Hou, H.L. Wang, and Y.G. Cheng, Investigation into the adsorption of CO_2, N_2 and CH_4 on kaolinite clay, *Arabian J. Chem.*, 15(2022), No. 3, art. No. 103665.

[51] K. Ramadass, G. Singh, K.S. Lakhi, *et al.*, Halloysite nanotubes: Novel and eco-friendly adsorbents for high-pressure CO_2 capture, *Microporous Mesoporous Mater.*, 277(2019), p. 229.

[52] J. Kim, I. Rubino, J.Y. Lee, and H.J. Choi, Application of halloysite nanotubes for carbon dioxide capture, *Mater. Res. Express*, 3(2016), No. 4, art. No. 045019.

[53] C. Chen, D.W. Park, and W.S. Ahn, Surface modification of a low cost bentonite for post-combustion CO_2 capture, *Appl. Surf. Sci.*, 283(2013), p. 699.

[54] N. Horri, E.S. Sanz- Pérez, A. Arencibia, R. Sanz, N. Frini-Srasra, and E. Srasra, Amine grafting of acid-activated bentonite for carbon dioxide capture, *Appl. Clay Sci.*, 180(2019), art. No. 105195.

[55] E. Vilarrasa-García, J.A. Cecilia, E.R. Aguado, *et al.*, Amino-modified pillared adsorbent from water-treatment solid wastes applied to CO_2/N_2 separation, *Adsorption*, 23(2017), No. 2, p. 405.

[56] G. Gómez-Pozuelo, E.S. Sanz-Pérez, A. Arencibia, P. Pizarro, R. Sanz, and D.P. Serrano, CO_2 adsorption on amine-functionalized clays, *Microporous Mesoporous Mater.*, 282(2019), p. 38.

[57] J.A. Cecilia, E. Vilarrasa-García, C.L. Cavalcante, D.C.S. Azevedo, F. Franco, and E. Rodríguez-Castellón, Evaluation of two fibrous clay minerals (sepiolite and palygorskite) for CO_2 capture, *J. Environ. Chem. Eng.*, 6(2018), No. 4, p. 4573.

[58] H. Zhu, S.M. Li, J.F. Zhang, L.K. Zhao, and Y. Huang, A highly effective and low-cost sepiolite-based solid amine adsorbent for CO_2 capture in post-combustion, *Sep. Purif. Technol.*, 306(2023), art. No. 122627.

[59] K. Quiroz-Estrada, M. Hernández-Espinosa, F. Rojas, R. Portillo, E. Rubio, and L. López, N_2 and CO_2 adsorption by soils with high kaolinite content from San Juan Amecac, Puebla, México, *Minerals*, 6(2016), No. 3, art. No. 73.

[60] T.F. Bates, F. Hildebrand, and A. Swineford, Morphology and structure of endellite and halloysite, *Am. Mineral.*, 35(1950), p. 463.

[61] Y.M. Lvov, D.G. Shchukin, H. Möhwald, and R.R. Price, Halloysite clay nanotubes for controlled release of protective agents, *ACS Nano*, 2(2008), No. 5, p. 814.

[62] A. Hamza, I.A. Hussein, M.J. Al-Marri, M. Mahmoud, and R. Shawabkeh, Impact of clays on CO_2 adsorption and enhanced gas recovery in sandstone reservoirs, *Int. J. Greenh. Gas Contr.*, 106(2021), art. No. 103286.

[63] W.B. Wang, B. Mu, J.P. Zhang, and A.Q. Wang, Attapulgite: From clay minerals to functional materials, *Sci. Sin. Chim*, 48(2018), No. 12, p. 1432.

[64] J. Ouyang, W. Gu, C.H. Zheng, *et al.*, Polyethyleneimine (PEI) loaded $MgO–SiO_2$ nanofibers from sepiolite minerals for reusable CO_2 capture/release applications, *Appl. Clay Sci.*, 152(2018), p. 267.

[65] W.L. Wang, J. Xiao, X.L. Wei, J. Ding, X.X. Wang, and C.S. Song, Development of a new clay supported polyethylenimine composite for CO_2 capture, *Appl. Energy*, 113(2014), p. 334.

[66] M.Y. Niu, H.M. Yang, X.C. Zhang, Y.T. Wang, and A.D. Tang, Amine-impregnated mesoporous silica nanotube as an emerging nanocomposite for CO_2 capture, *ACS Appl. Mater. Interfaces*, 8(2016), No. 27, p. 17312.

[67] Ouyang, C.H. Zheng, W. Gu, Y. Zhang, H.M. Yang, and S.L. Suib, Textural properties determined CO_2 capture of tetraethylenepentamine loaded SiO_2 nanowires from α-sepiolite, *Chem. Eng. J.*, 337(2018), p. 342.

[68] S. Barakan and V. Aghazadeh, The advantages of clay mineral modification methods for enhancing adsorption efficiency in wastewater treatment: A review, *Environ. Sci. Pollut. Res. Int.*, 28(2021), No. 3, p. 2572.

[69] Z.L. Huang, D. Karami, and N. Mahinpey, Study on the efficiency of multiple amino groups in ionic liquids on their sorbents performance for low-temperature CO_2 capture, *Chem. Eng. Res. Des.*, 167(2021), p. 198.

[70] G.T. Rochelle, Amine scrubbing for CO_2 capture, *Science*, 325(2009), No. 5948, p. 1652.

[71] U. Bhatti, D. Sivanesan, S. Nam, S.Y. Park, and I.H. Baek, Efficient $Ag_2O–Ag_2CO_3$ catalytic cycle and its role in minimizing the energy requirement of amine solvent regeneration for

CO_2 capture, *ACS Sustainable Chem. Eng.*, 7(2019), No. 12, p. 10234.

[72] A. Veawab, P. Tontiwachwuthikul, and A. Chakma, Corrosion behavior of carbon steel in the CO_2 absorption process using aqueous amine solutions, *Ind. Eng. Chem. Res.*, 38(1999), No. 10, p. 3917.

[73] P.F. Xie, L.Q. Li, Z.C. He, and C.Q. Su, Gas-liquid mass transfer of carbon dioxide capture by magnesium hydroxide slurry in a bubble column reactor, *J. Cent. South Univ.*, 26(2019), No. 6, p. 1592.

[74] F.S. Taheri, A. Ghaemi, A. Maleki, and S. Shahhosseini, High CO_2 adsorption on amine-functionalized improved mesoporous silica nanotube as an eco-friendly nanocomposite, *Energy Fuels*, 33(2019), No. 6, p. 5384.

[75] J. Ouyang, W. Gu, Y. Zhang, *et al.*, CO_2 capturing performances of millimeter scale beads made by tetraethylenepentamine loaded ultra-fine palygorskite powders from jet pulverization, *Chem. Eng. J.*, 341(2018), p. 432.

[76] C. Chen, J. Kim and W.-S. Ahn, CO_2 capture by amine-functionalized nanoporous materials: A review, *Korean J. Chem. Eng.*, 31(2014), No. 11, p. 1919.

[77] H.H. Cai, F. Bao, J. Gao, T. Chen, S. Wang, and R. Ma, Preparation and characterization of novel carbon dioxide adsorbents based on polyethylenimine-modified halloysite nanotubes, *Environ. Technol.*, 36(2015), No. 9-12, p. 1273.

[78] M. Irani, M.H. Fan, H. Ismail, A. Tuwati, B. Dutcher, and A.G. Russell, Modified nanosepiolite as an inexpensive support of tetraethylenepentamine for CO_2 sorption, *Nano Energy*, 11(2015), p. 235.

[79] W.L. Wang, X.X. Wang, C.S. Song, X.L. Wei, J. Ding, and J. Xiao, Sulfuric acid modified bentonite as the support of tetraethylenepentamine for CO_2 capture, *Energy Fuels*, 27(2013), No. 3, p. 1538.

[80] E. Vilarrasa-García, J.A. Cecilia, D.C.S. Azevedo, C.L. Cavalcante, and E. Rodríguez-Castellón, Evaluation of porous clay heterostructures modified with amine species as adsorbent for the CO_2 capture, *Microporous Mesoporous Mater.*, 249(2017), p. 25.

[81] M. Atilhan, S. Atilhan, R. Ullah, *et al.*, High-pressure methane, carbon dioxide, and nitrogen adsorption on amine-impregnated porous montmorillonite nanoclays, *J. Chem. Eng. Data*, 61(2016), No. 8, p. 2749.

[82] G. Singh, K.S. Lakhi, I.Y. Kim, *et al.*, Highly efficient method for the synthesis of activated mesoporous biocarbons with extremely high surface area for high-pressure CO_2 adsorption, *ACS Appl. Mater. Interfaces*, 9(2017), No. 35, p. 29782.

[83] L.L. He, M.H. Fan, B. Dutcher, *et al.*, Dynamic separation of ultradilute CO_2 with a nanoporous amine-based sorbent, *Chem. Eng. J.*, 189-190(2012), p. 13.

[84] S. Chen, B. Jia, Y. Peng, *et al.*, CO_2 adsorption behavior of 3-aminopropyltrimethoxysilane-functionalized attapulgite with the grafting modification method, *Ind. Eng. Chem. Res.*, 60(2021), No. 47, p. 17150.

[85] S. Park, J. Ryu, H.Y. Cho, and D. Sohn, Halloysite nanotubes loaded with HKUST-1 for CO_2 adsorption, *Colloids Surf. A*, 651(2022), art. No. 129750.

[86] L. Stevens, K. Williams, W.Y. Han, *et al.*, Preparation and CO_2 adsorption of diamine modified montmorillonite via exfoliation grafting route, *Chem. Eng. J.*, 215-216(2013), p. 699.

[87] S. Chen, Y.N. Chao, J.M. Wu, H. Ye, X. Luo, and Z.W. Liang, A new solid adsorbent for CO_2 capture based on an amine polycarboxylate ionic liquid with multiple absorption sites, *Ind. Eng. Chem. Res.*, 61(2022), No. 32, p. 11953.

[88] S.Z. Hu and H.L. Zhang, Analysis of CO_2 adsorption performance of ionic liquid modified halloysite, *Ion Exch. Adsorpt.*, 37(2021), No. 6, p. 543.

[89] L.A. Galeano, M.Á. Vicente, and A. Gil, Catalytic degradation of organic pollutants in aqueous streams by mixed Al/M-pillared clays (M = Fe, Cu, Mn), *Catal. Rev. Sci. Eng.*, 56(2014), No. 3, p. 239.

[90] J.T. Kloprogge, Synthesis of smectites and porous pillared clay catalysts: A review, *J. Porous Mater.*, 5(1998), No. 1, p. 5.

[91] K. Wu, Q. Ye, R.P. Wu, S. Chen, and H.X. Dai, Carbon dioxide adsorption behaviors of aluminum-pillared montmorillonite-supported alkaline earth metals, *J. Environ. Sci.*, 98(2020), p. 109.

[92] K. Wu, Q. Ye, R.P. Wu, and H.X. Dai, Alkali metal-promoted aluminum-pillared montmorillonites: High-performance CO_2 adsorbents, *J. Solid State Chem.*, 291(2020), art. No. 121585.

[93] R. Sanz, G. Calleja, A. Arencibia, and E.S. Sanz-Pérez, Development of high efficiency adsorbents for CO_2 capture based on a double-functionalization method of grafting and impregnation, *J. Mater. Chem. A*, 1(2013), No. 6, p. 1956.

[94] W. Seifritz, CO_2 disposal by means of silicates, *Nature*, 345(1990), No. 6275, art. No. 486.

[95] K.S. Lackner, C.H. Wendt, D.P. Butt, E.L. Joyce, and D.H. Sharp, Carbon dioxide disposal in carbonate minerals, *Energy*, 20(1995), No. 11, p. 1153.

[96] W.J. Ding, J. Ouyang, and H.M. Yang, Synthesis and characterization of nesquehonite ($MgCO_3 \cdot 3H_2O$) powders from natural talc, *Powder Technol.*, 292(2016), p. 169.

[97] K.S. Lackner, D.P. Butt, and C.H. Wendt, Progress on binding CO_2 in mineral substrates, *Energy Convers. Manage.*, 38(1997), p. S259.

[98] W.K. O'Connor, D.C. Dahlin, G.E. Rush, C.L. Dahlin, and W.K. Collins, Carbon dioxide sequestration by direct mineral carbonation: Process mineralogy of feed and products, *Min. Metall. Explor.*, 19(2002), No. 2, p. 95.

[99] W.J.J. Huijgen, G.J. Witkamp, and R.N.J. Comans, Mechanisms of aqueous wollastonite carbonation as a possible CO_2 sequestration process, *Chem. Eng. Sci.*, 61(2006), No. 13, p. 4242.

[100] C.Y. Tai, W.R. Chen, and S.M. Shih, Factors affecting wollastonite carbonation under CO_2 supercritical conditions, *AlChE J.*, 52(2006), No. 1, p. 292.

[101] R. Zevenhoven, A. Wiklund, J. Fagerlund, *et al.*, Carbonation of calcium-containing mineral and industrial by-products, *Front. Chem. Eng. China*, 4(2010), No. 2, p. 110.

[102] A.A. Fara, M.R. Rayson, G.F. Brent, T.K. Oliver, M. Stockenhuber, and E.M. Kennedy, Formation of magnesite and hydromagnesite from direct aqueous carbonation of thermally activated lizardite, *Environ. Prog. Sustainable Energy*, 38(2019), No. 3, art. No. e13244.

[103] F. Farhang, T.K. Oliver, M. Rayson, G. Brent, M. Stockenhuber, and E. Kennedy, Experimental study on the precipitation of magnesite from thermally activated serpentine for CO_2 sequestration, *Chem. Eng. J.*, 303(2016), p. 439.

[104] M. Fabian, M. Shopska, D. Paneva, *et al.*, The influence of attrition milling on carbon dioxide sequestration on magnesium–iron silicate, *Miner. Eng.*, 23(2010), No. 8, p. 616.

[105] J.J. Li and M. Hitch, Mechanical activation of magnesium silicates for mineral carbonation, a review, *Miner. Eng.*, 128(2018), p. 69.

[106] W.J.J. Huijgen, G.J. Ruijg, R.N.J. Comans, and G.J. Witkamp, Energy consumption and net CO_2 sequestration of aqueous mineral carbonation, *Ind. Eng. Chem. Res.*, 45(2006), No. 26, p. 9184.

[107] S.J. Gerdemann, W.K. O'Connor, D.C. Dahlin, L.R. Penner, and H. Rush, *Ex situ* aqueous mineral carbonation, *Environ. Sci. Technol.*, 41(2007), No. 7, p. 2587.

[108] E. Eikeland, A.B. Blichfeld, C. Tyrsted, A. Jensen, and B.B. Iversen, Optimized carbonation of magnesium silicate mineral

for CO_2 storage, *ACS Appl. Mater. Interfaces*, 7(2015), No. 9, p. 5258.

[109] J.J. Li, A.D. Jacobs, and M. Hitch, Direct aqueous carbonation on olivine at a CO_2 partial pressure of 6.5 MPa, *Energy*, 173(2019), p. 902.

[110] S. Teir, R. Kuusik, C.J. Fogelholm, and R. Zevenhoven, Production of magnesium carbonates from serpentinite for long-term storage of CO_2, *Int. J. Miner. Process.*, 85(2007), No. 1-3, p. 1.

[111] G.L.A.A. Ferrufino, S. Okamoto, J.C.D. Santos, *et al.*, CO_2 sequestration by pH-swing mineral carbonation based on HCl/NH_4OH system using iron-rich lizardite 1T, *J. CO_2 Util.*, 24(2018), p. 164.

[112] X.L. Wang and M.M. Maroto-Valer, Dissolution of serpentine using recyclable ammonium salts for CO_2 mineral carbonation, *Fuel*, 90(2011), No. 3, p. 1229.

[113] J. Fagerlund, E. Nduagu, I. Romão, and R. Zevenhoven, CO_2 fixation using magnesium silicate minerals part 1: Process description and performance, *Energy*, 41(2012), No. 1, p. 184.

[114] W.J. Bao, H.Q. Li, and Y. Zhang, Experimental investigation of enhanced carbonation by solvent extraction for indirect CO_2 mineral sequestration, *Greenh. Gases Sci. Technol.*, 4(2014), No. 6, p. 785.

[115] F. Goff and K.S. Lackner, Carbon dioxide sequestering using ultramaf IC rocks, *Environ. Geosci.*, 5(1998), No. 3, p. 89.

[116] H.J. Ziock, D.P. Butt, K.S. Lackner, and C.H. Wendt, The need and options available for permanent CO_2 disposal, [in] M.A. Abraham and R.P. Hesketh, eds., *Reaction Engineering for Pollution Prevention*, Elsevier, Amsterdam, 2000, p. 41.

[117] S. Teir, H. Revitzer, S. Eloneva, C.J. Fogelholm, and R. Zevenhoven, Dissolution of natural serpentinite in mineral and organic acids, *Int. J. Miner. Process.*, 83(2007), No. 1-2, p. 36.

[118] W.K. O'Connor, D.C. Dahlin, D.N. Nilsen, G.E. Rush, R.P. Walters, and P.C. Turner, CO_2 storage in solid form: A study of direct mineral carbonation, [in] *5th International Conference on Greenhouse Gas Technologies*, Cairns, 2000, p. 14.

[119] W.J.J. Huijgen, *Carbon Dioxide Sequestration by Mineral Carbonation*, Wageningen University and Research, Wageningen, 2007, p. 47.

[120] B. Metz, O. Davidson, H. de Coninck, M. Loos, and L. Meyer, *IPCC Special Report*: *Carbon Dioxide Capture and Storage*, Cambridge University Press, Cambridge, 2005, p. 323.

[121] J.G. Blencoe, D.A. Palmer, L.M. Anovitz, and J.S. Beard, *Carbonation of Metal Silicates for Long-Term* CO_2 *Sequestration*, United States Patent, Appl. 13/361215, 2014.

[122] E. Nduagu, T. Björklöf, J. Fagerlund, *et al.*, Production of magnesium hydroxide from magnesium silicate for the purpose of CO_2 mineralization – Part 2: Mg extraction modeling and application to different Mg silicate rocks, *Miner. Eng.*, 30(2012), p. 87.

[123] I.S. Romão, L.M. Gando-Ferreira, and R. Zevenhoven, Combined extraction of metals and production of $Mg(OH)_2$ for CO_2 sequestration from nickel mine ore and overburden, *Miner. Eng.*, 53(2013), p. 167.

[124] W. Raza, N. Raza, H. Agbe, R.V. Kumar, K.H. Kim, and J.H. Yang, Multistep sequestration and storage of CO_2 to form valuable products using forsterite, *Energy*, 155(2018), p. 865.